New Design of Falling Film Evaporator

CHITTAPOL SOOKSANIT

A Report Submitted in Partial Fulfillment of the Requirements

for the Degree of Bachelor of Engineering (Petrochemical Engineering)

Department of Chemical Engineering, Faculty of Engineering,

King Mongkut's Institute of Technology Ladkrabang

Academic Year 2017

การออกแบบเครื่องระเหยแบบฟิล์มเคลื่อนที่ลงแบบใหม่

ชิตพล สุขสนิท

ปริญญานิพนธ์นี้เป็นส่วนหนึ่งของการศึกษาตามหลักสูตร

วิศวกรรมศาสตรบัณฑิต สาขาวิชาวิศวกรรมปิโตรเคมี

ภาควิชาวิศวกรรมเคมี คณะวิศวกรรมศาสตร์

สถาบันเทคโนโลยีพระจอมเกล้าเจ้าคุณทหารลาดกระบัง

ปีการศึกษา 2560

Title	New Design of Falling Film Evaporator
By	Mr. Chittapol Sooksanit
Field of Study	Petrochemical Engineering
Advisor	Asst. Prof. Dr. Nuttapol Lerkkasemsan

Accepted by the Faculty of Engineering, King Mongkut's Institute of Technology Ladkrabang in Partial Fulfillment of the Requirements for the Degree of Bachelor of Engineering (Petrochemical Engineering).

Thesis Committee

_____ Chairman
(Asst. Prof. Dr. Nuttapol Lerkkasemsan)

_____ Committee
(Asst. Prof. Dr. Apinan Namkanisorn)

_____ Committee
(Asst. Prof. Ruenruedee Benjangkaprasert)

Title	New Design of Falling Film Evaporator
By	Mr. Chittapol Sooksanit
Advisor	Asst. Prof. Dr. Nuttapol Lerkkasemsan
Field of Study	Petrochemical Engineering
Affiliation	Department of Chemical Engineering

Abstract

This study aims to develop the new design of falling film evaporator, the purpose is to reduce the effect of pressure drop in tube. Feed is the thin film of sugar solution that appears at the outer surface of the hot tube and is operated at 50 mmHg. Hot water is counter current flow inside the hot tube. Firstly, temperature and concentration profiles of the falling film are observed by a numerical method, the system needs the principles of heat and mass transfer simultaneously, it could be calculated by MATLAB program. Factors of the falling film evaporator is similar to shell and tube heat exchanger, pressure drop measurement could be based on the shell and tube heat exchanger calculation. Another important part is the heating media system, the hot tube contains a small tube inside it, and material of the hot tube should be better in heat conduction than shell and sub-tube material. FLUENT program leads easier observation of temperature and velocity profiles of fluid flow in pipe. The criteria of designing which used to analyze and design the new ways are the energy consumed worthiness and over 25% of rate of evaporation. The optimal system could produce the 20.0234 wt% of sugar solution from 15 wt% and rate of evaporation is 25.0876 %.

Keywords: Falling film evaporator, Vacuum system, Shell and tube

เรื่อง การออกแบบเครื่องระเหยแบบฟิล์มเคลื่อนที่ลงแบบใหม่
โดย นายชิตพล สุขสนิท
อาจารย์ที่ปรึกษา ผศ. ดร. ณัฐพล ฤกษ์เกษมสันต์
สาขาวิชา วิศวกรรมปิโตรเคมี
สังกัด วิศวกรรมปิโตรเคมี

บทคัดย่อ

การศึกษานี้เป็นการออกแบบเครื่องระเหยแบบฟิล์มเคลื่อนที่ลงแบบใหม่เพื่อลดผลกระทบของความดันตกภายในท่อ โดยสารละลายน้ำตาลจะถูกป้อนเป็นแผ่นฟิล์มบาง ๆ ภายนอกท่อในสภาวะสุญญากาศ 50 มิลลิเมตรปรอทและถูกให้ความร้อนด้วยน้ำร้อนที่ไหลสวนทางกันซึ่งอยู่ภายในท่อ โดยขั้นแรกเริ่มจากการศึกษาการรายละเอียดอุณหภูมิและความเข้มข้นในแผ่นฟิล์มและใช้ระเบียบวิธีเชิงตัวเลขมามาช่วยในการศึกษาการถ่ายเทมวลและความร้อนที่เกิดขึ้นพร้อม ๆ กันโดยผ่านโปรแกรม MATLAB เครื่องระเหยแบบฟิล์มเคลื่อนที่ลงจะมีปัจจัยในการศึกษาคล้าย ๆ กับเครื่องแลกเปลี่ยนความร้อนชนิดเชลล์และท่อ ทำให้การคำนวณในส่วนของความดันตกในส่วนเชลล์ถูกคิดในลักษณะคล้ายกับเครื่องแลกเปลี่ยนความร้อนชนิดเชลล์และท่อ สิ่งที่สำคัญอีกสิ่งหนึ่งของการศึกษานี้คือระบบให้ความร้อน ภายในท่อจะประกอบด้วยท่อเล็กซึ่งอยู่ภายในอีก 1 ท่อ และวัสดุของท่อภายนอกจะเป็นท่อที่นำความร้อนได้ดีกว่าวัสดุส่วนของเชลล์และท่อเล็กภายใน โปรแกรม FLUENT ช่วยในการศึกษารายละเอียดอุณหภูมิและความเร็วของของไหลภายในท่อได้เป็นอย่างดี โดยหลักเกณฑ์ที่จะนำมาใช้ในการวิเคราะห์และออกแบบคือความคุ้มค่าของพลังงานที่ใช้และมีอัตราการระเหยที่มากกว่าร้อยละ 25 ซึ่งผลการศึกษาระบบออกแบบสามารถทำให้สารละลายน้ำตาลจากความเข้มข้นร้อยละ 15 โดยมวล เป็นความเข้มข้นร้อยละ 20.0234 โดยมวล โดยมีอัตราการระเหยอยู่ที่ร้อยละ 25.0876

คำสำคัญ: เครื่องระเหยแบบฟิล์มเคลื่อนที่ลง, สภาวะสุญญากาศ, เชลล์และท่อ

Acknowledgements

This thesis has been proceeded step by step to the achievement. I would like to express my grateful thanks to my advisor, Asst. Prof. Dr. Nuttapol Lerkkasemsan for his useful help and encouragement. I am very appreciated for his advice, not only the research methodologies but also many plan of life. I could not have completed this thesis without all the supports that I have been taking from him.

In addition, I am grateful for all personnel of department of Chemical Engineering, King Mongkut's Institute of Technology Ladkrabang, for suggestions and all their help. Finally, I most gratefully acknowledge my parents and my friends for all support throughout the timing of this research.

Chittapol Sooksanit

Table of Contents

Page

Table of Contents (Cont.)

List of Figures

Page

List of Figures (Cont.)

Page

List of Figures (Cont.)

Page

List of Tables

Page

CHAPTER I
INTRODUCTION

1.1 Background

Falling film evaporator has been played a role in several industrials[1], especially food and pharmaceutical industrials. It can increase the concentration of a high viscous solution and low temperature requirement. The simple using and lower temperature operation are good choices to study this falling film evaporator. Generally, feed falling film appears inside of hot tubes, and the outside is heating media. Some vegetable or fruit juices cannot stand with high temperature, then the falling film evaporator which usually does not be operated at high temperature is one of a proper type used to increase the concentration of these samples. However, it needs a continuous and uniform distribution of the feed falling film and low feed flow rate, involving with Reynolds number, laminar flow with pronounced rippling or turbulent flow would occur if Re > 1500. The high feed flow rate causes the large thickness of the falling film and rate of evaporation would decrease. Wei et al. [2] investigated the newly-designed enhanced tube bundle in a vacuum condition provided better heat transfer performance even high flow rate, the pronounced rip on flow causes rough flow and discrete temperature distribution. Furthermore, the evaporation accumulates vapors surely, that is the subsequence of pressure drop inside the hot tube and decreasing of its effectiveness. These problems are interesting about how to eliminate the effects and enhance them. [3] The study on the absorption of water vapor could explain the profiles of concentration and temperature by a numerical method. Concentration and temperature profiles were studied by dividing the film to small grids and approximation of unknown by a numerical method. Heat and mass transfer of each small grids and layers were considered simultaneously to relate the various factors and be led to explain the falling film characteristics, energy requirement, and evaporation phenomena.

A study of the modeling of an evaporator[4], was explained the phenomena of the falling film and concentrated to construct a model with the new design of falling film evaporator to eliminate the previous problems. The feed falling film appeared at the outside of the hot tube surface as a new design. This study aims to develop this model and calculate more various factors that affect to evaporation as optimization for a bigger system studying.

1.2 Objectives

1.2.1 To develop the model of falling film evaporator

1.2.2 To study the factors of falling film characteristics to optimization

1.2.3 To construct a mathematical model to predict the evaporation phenomena of falling film evaporator

1.3 Scopes of Work

1.3.1 Optimize the factors which direct to the outlet concentrated product such feed flow rate, temperature of heating media and dimension of hot tubes

1.3.2 Construct the mathematical model to design a new design of falling film evaporator from the feed step to product step

1.4 Expected Outputs

1.4.1 Understand the overall system both heat and mass transfers involving to falling film

1.4.2 Take the complete calculation model of the new design of falling film evaporator

CHAPTER II
LITERATURE REVIEW

2.1 Falling Film Evaporator

Falling film evaporator is a long tube evaporator with vertical shell and tube heat exchanger[5]. Its main principles are feed liquid as a thin film to increase surface area, and operate under vacuum system to reduce input energy, industrial scales take the heating media around 60 -70 °C of inlet temperature of the heating media. Feed is usually taken a preliminary or preheat step before evaporation step to economical production with optimal conditions. Feed liquid to be concentrated appears to the top of a heating tube, the thin film feed liquid is always continuously distributed. Generally, vapor and residue feed liquid are separated downward part.

It would be difficult to control and study the feed film liquid profiles if the film velocity and film thickness depend on time, the slow and continuous flow can be supported by a distributor to make sure that the feed film liquids got uniform movement around the tube. The falling film evaporator is shown below in Figure 2.1.

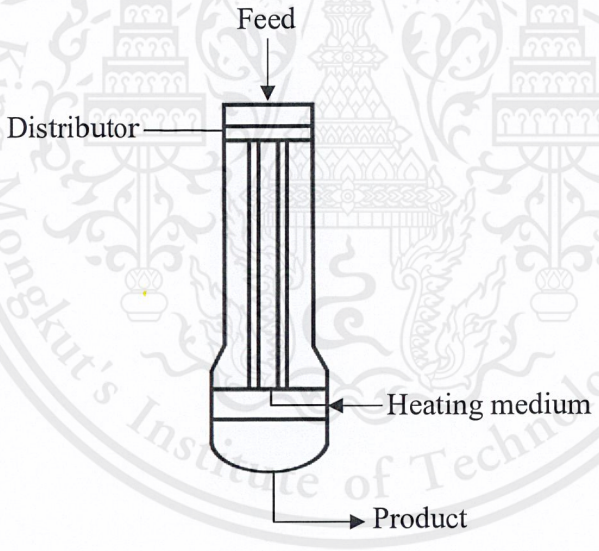

Figure 2.1 Falling film evaporator

2.2 Falling Film Characteristics

2.2.1 System Analysis Assumptions

Energy requirement for the system needs the energy sufficiency to completely evaporate at the surface of the thin film, so the falling film must be slow downward by gravity. The film thickness is kept being smaller by continuous evaporation. This model is simply constructed with 2-dimension cartesian coordinate. In Figure 2.2, x-coordinate is defined downstream along the tube and y-coordinate is defined cross-stream along the film thickness by the following assumptions:

1. Diameter of tube is very large compared to the film thickness, the heat and mass transfer in angular direction is neglected
2. Feed flows in the horizontal perimeter are equivalent
3. Constant density of feed liquid is considered
4. No bulk fluid motion, diffusion and heat convection in both directions occur
5. Feed liquid is viscous and no-slip wall boundary appears
6. Feed liquid is laminar flow with non-wavy throughout
7. Wall thickness of tube is neglected

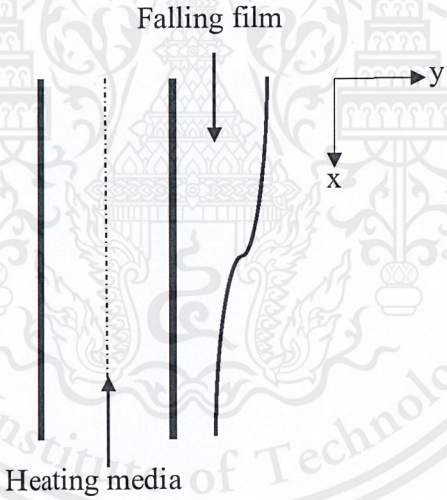

Figure 2.2 Falling film characteristics

2.2.2 Variables

[3] Newtonian fluid with laminar flow is considered in 2-dimension of the equation of motion for a fluid with both constant density and viscosity, which is

$$\mu \frac{\partial^2 u}{\partial y^2} = -\rho g \tag{2.2.1}$$

with the initial and boundary conditions: at y = 0, u = 0 and $y = \delta, \frac{du}{dy} = 0$ (2.2.2)

The equation of motion is solved with boundary conditions (2.2.2) in x-direction

$$u = \frac{\rho g \delta^2}{2\mu}\left[2\left(\frac{y}{\delta}\right) - \left(\frac{y}{\delta}\right)^2\right] \tag{2.2.3}$$

For y-direction, velocity can be defined by continuity equation:

$$v = -\frac{gy^2}{2\upsilon}\frac{d\delta}{dx} \tag{2.2.4}$$

Film Reynolds number is a necessary parameter to consideration of falling film characteristics, laminar film flow with little wavy or non- wavy are taken uniform and continuous distribution [6].

Laminar flow with negligible rippling	Re < 20
Laminar flow with pronounced rippling	20 < Re < 1500
Turbulent flow	Re > 1500

Film Reynolds number: $\mathrm{Re} = \frac{4\Gamma}{\mu}$ (2.2.5)

However, it can be defined film Reynolds number in term of velocity:

$$\mathrm{Re} = \frac{4\rho \bar{u} \delta}{\mu} \tag{2.2.6}$$

Film thickness: $\delta = \left(\frac{3\Gamma\mu}{g\rho}\right)^{1/3}$ (2.2.7)

where x position in x-direction, m

y position in y-direction, m

μ viscosity of film, $kg.m^{-1}s^{-1}$

ρ film density, kg/m^3

u film velocity in x-direction, m/s

v film velocity in y-direction, m/s

$\bar{u}$ average film velocity in x-direction, m/s

g gravitational acceleration, m/s^2

δ film thickness, m

Γ film flow rate, $kg.m^{-1}\ s^{-1}$

Re film Reynolds number, dimensionless

2.3 Heat Transfer of Film

The source of energy is from heating media as a hot water, it needs the sufficient energy for evaporation at the film surface. The input energy of heating media is gradually transferred from the inner tube wall to outer as conduction, then conducts to the film surface, evaporation would occur if the amount of energy reaches to the latent heat of vaporization.

This study is assumed that the wall thickness is very small, heat transfer inside the tube wall is very small effects compared to the latent heat of vaporization. The rate of evaporation could be increased if the system is taken the higher inlet temperature of heating media, but more energy is also wasted consumed. The system is described in term of energy balance:

Energy input (Q_1) = Heat conduction of film (Q_2) + Heat of vaporization (Q_3) (2.3.1)

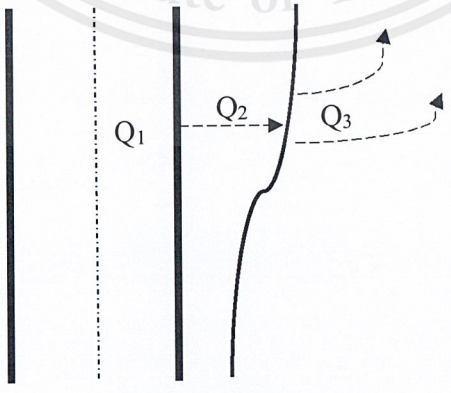

Figure 2.3 Energy balance

Heat conduction of film (Q_2): $$q = -k_f \frac{dT}{dy} \quad (2.3.2)$$

Film velocity in x-direction greatly impacts to the system analysis, this study does not be recognized to diffusion and bulk fluid motion at the falling film, it is only shown in term of heat conduction in equation (2.3.1).

Latent heat of vaporization (Q_3): $$q = m_e h_{fg} \quad (2.3.3)$$

And at the vapor-liquid interface [7]

$$k_f \left.\frac{\partial T}{\partial y}\right|_{y=\delta} = h_{fg} \frac{\rho D_m}{1-\omega_s} \left.\frac{\partial \omega}{\partial y}\right|_{y=\delta} \quad (2.3.4)$$

Given q heat flux, $W.m^{-2}K^{-1}s^{-1}$
k_f thermal conductivity of film, $W.m^{-1}K^{-1}$
T temperature, K
m_e evaporated mass flux, kg m^{-2} s^{-1}
h_{fg} heat of vaporization, J/kg
D_m Diffusion coefficient, m^2/s
ω Concentration of sugar solution, wt%
ω_s Concentration of sugar solution at the film surface, wt%

2.4 Mass Transfer of Film

2.4.1 Evaporation

Evaporation appears at the film surface when heat transfer is proceeded to the film surface, the solvent mass is evaporated by the latent heat of vaporization, then film surface concentration is immediately increased as the solvent mass elimination or evaporation. We modified the relation of film surface concentration and rate of evaporation from equation (2.3.4) as follows:

$$m_e = \frac{\rho D_m}{(1-\omega_s)} \frac{d\omega}{dy} \quad (2.4.1)$$

2.4.2 Vapor-Liquid Equilibrium

This topic is the main study which is very important to consider and analyze the overall system of the new design of evaporator, it can indicate the effectiveness of rate of evaporation

for each operated condition. It is a static condition which no changes appear of the system with time. The equilibrium balance between vapor and liquid at the surface is then considered.

The Antoine equation is based on an exact thermodynamic relationship between the properties of different phases, the thermodynamic properties of pressure and temperature could be explained it when its properties approach a saturated liquid. That is followed by

Antoine equation:

$$\ln P^{sat} = A - \frac{B}{T - C} \tag{2.4.2}$$

where A, B, and C are Antoine equation's constant. However, the previous relation is for a pure liquid, it needs some mixed properties to an adaptable application.

Raoult's law can support the studying of a saturated pressure of mixed solution under the conditions of vapor phase and liquid phase which are ideal gas and ideal solution, respectively. However, this system is operated under the vacuum condition which is in keeping with the two assumptions. [8]

Raoult's law

$$y_i P = x_i P_i^{sat} \tag{2.4.3}$$

The equation (2.4.3) would be used with component i of the mixed solution, where P is system pressure, P^{sat} is saturated pressure, x and y are liquid and vapor mole fraction, respectively. The equation (2.4.3) is transformed to modified Raoult's law (2.4.4) for the mixed solution of component 1 and component 2.

$$P = P_2^{sat} + (P_1^{sat} - P_2^{sat})x_1 \tag{2.4.4}$$

2.5 Concentration and Temperature Profiles

Evaporation is an endothermic process, energy is applied from inside the film to the surface. The film surface temperature is then lower than inside, and the surface region is got higher concentration.

The progress to create the new design of falling film evaporator needs to know the both profiles, the calculations would be solved to enhance the equipment and system.

Energy equation:

$$u\frac{\partial T'}{\partial x} + v\frac{\partial T'}{\partial y} = \alpha\frac{\partial^2 T'}{\partial y^2} \tag{2.5.1}$$

Quality equation:

$$u\frac{\partial w}{\partial x} + v\frac{\partial w}{\partial y} = D_m\frac{\partial^2 w}{\partial y^2} \tag{2.5.2}$$

The temperature and concentration profiles can be explained by both equations (2.5.1) and (2.5.2), respectively. We need initial and boundary conditions to solve these differential equations and get the general form.

The initial and boundary conditions of energy equation (2.5.1):

1) At the feed inlet tube $x = 0,\ T = T_{feed}$
2) At the outer wall $y = 0,\ T = T_{wall}$

The initial and boundary conditions of quality equation (2.5.2):

1) At the feed inlet tube $x = 0,\ \omega = \omega_{feed}$
2) At the outer wall $y = 0,\ \frac{d\omega}{dy} = 0$

Given α thermal diffusivity of sugar solution, m^2/s

$$\alpha = \frac{k_s}{\rho C_p}$$

2.6 Numerical Method

The differential equations (2.5.1) and (2.5.2) are solved by transforming the x and y directions to non-dimensional x and y axis [3] because the film thickness is gradually smaller followed the tube length by the evaporation. That is shown below in Figure 2.4

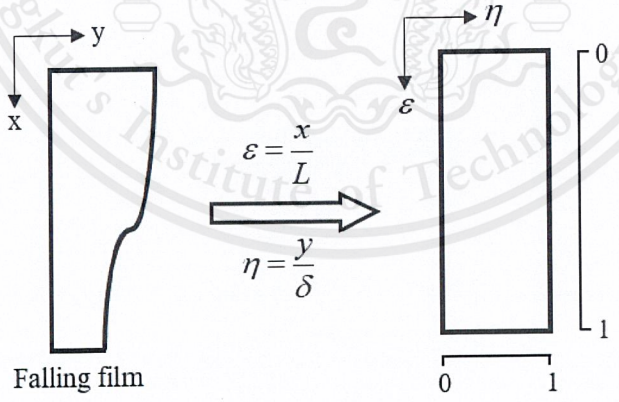

Figure 2.4 Transformation to non-dimensional axis

Given ε is non-dimensional x-axis

η is non-dimensional y-axis

The newly transformed equations are shown in equations (2.6.1) and (2.6.2), respectively.

$$\frac{\partial T}{\partial \varepsilon} = \left(\frac{\eta}{\delta} \frac{d\delta}{d\varepsilon} - \frac{vL}{u\delta} \right) \frac{\partial T}{\partial \eta} + \frac{\alpha L}{u\delta^2} \frac{\partial^2 T}{\partial \eta^2} \tag{2.6.1}$$

$$\frac{\partial \omega}{\partial \varepsilon} = \left(\frac{\eta}{\delta} \frac{d\delta}{d\varepsilon} - \frac{vL}{u\delta} \right) \frac{\partial \omega}{\partial \eta} + \frac{D_m L}{u\delta^2} \frac{\partial^2 \omega}{\partial \eta^2} \tag{2.6.2}$$

We divide the thin film to by many gridlines, the size of the small grids is MxN that would be shown in Figure 2. 5. The large number takes the more accurate prediction, but it would take a long time for calculation.

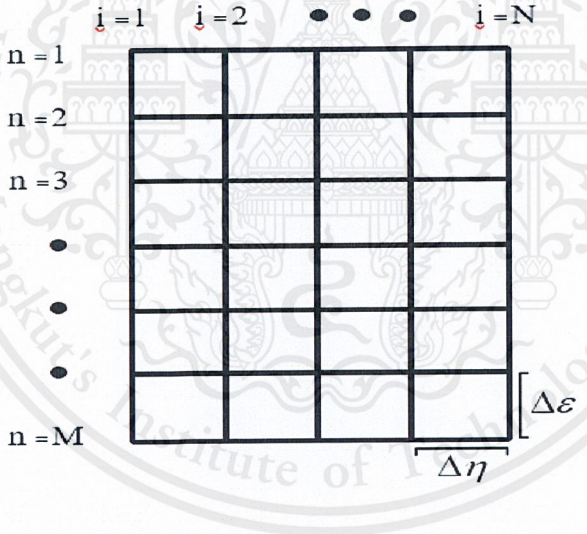

Figure 2.5 Grids division of falling film for M rows and N columns

- The first row (n = 1) is denoted the feed layer.
- The last row (n = M) is denoted the product layer.
- The first column (i = 1) is denoted the tube wall.
- The last column (i = N) is denoted the film surface.

The numerical method is involved the differentiation method, unknown approximation values are from the adjacent and close values. This study exemplifies on only differential equation (2.6.1) since the form of equations (2.6.1) and (2.6.2) is identical form,

Forward difference method:

$$\frac{\partial T}{\partial \varepsilon} = \frac{T_i^{n+1} - T_i^n}{\Delta \varepsilon} \tag{2.6.3}$$

$$\frac{\partial T}{\partial \eta} = \frac{T_{i+1}^n - T_i^n}{\Delta \eta} \tag{2.6.4}$$

Central difference method:

$$\frac{\partial^2 T}{\partial \eta^2} = \frac{T_{i+1}^n - 2T_i^n + T_{i-1}^n}{(\Delta \eta)^2} \tag{2.6.5}$$

Therefore, we can substitute the equations (2.6.3) to (2.6.5) in equation (2.6.1), that is

$$\frac{T_i^{n+1} - T_i^n}{\Delta \varepsilon} = \left(\frac{\eta}{\delta}\frac{d\delta}{d\varepsilon} - \frac{vL}{u\delta}\right)\left(\frac{T_{i+1}^n - T_i^n}{\Delta \eta}\right) + \frac{\alpha L}{u\delta^2}\left(\frac{T_{i+1}^n - 2T_i^n + T_{i-1}^n}{(\Delta \eta)^2}\right) \tag{2.6.6}$$

Equation (2.6.6) is transformed to the general form of equation (2.6.7), in the same way, the quality equation (2.5.2) is transformed to equation (2.6.8).

$$T_i^{n+1} = (B)T_{i-1}^n + (1 - A - 2B)T_i^n + (A + B)T_{i+1}^n \tag{2.6.7}$$

$$\omega_i^{n+1} = (B)\omega_{i-1}^n + (1 - A - 2C)\omega_i^n + (A + C)\omega_{i+1}^n \tag{2.6.8}$$

Given $A = \left(\frac{\eta}{\delta}\frac{d\delta}{d\varepsilon} - \frac{vL}{u\delta}\right)\frac{\Delta \varepsilon}{\Delta \eta}$

$$B = \left(\frac{\alpha L}{u\delta^2}\right)\frac{\Delta \varepsilon}{(\Delta \eta)^2}$$

$$C = \left(\frac{D_m L}{u\delta^2}\right)\frac{\Delta \varepsilon}{(\Delta \eta)^2}$$

From equations (2.6.7) and (2.6.8), we could calculate the values in row n+1, if the values in row n are formerly defined and kept doing until the last row finished.

Three-point values in an adjacent upper row would be used to calculate a lower one. The equations (2.6.7) and (2.6.8) could be considered and compared to Figure 2.6 to easily understand.

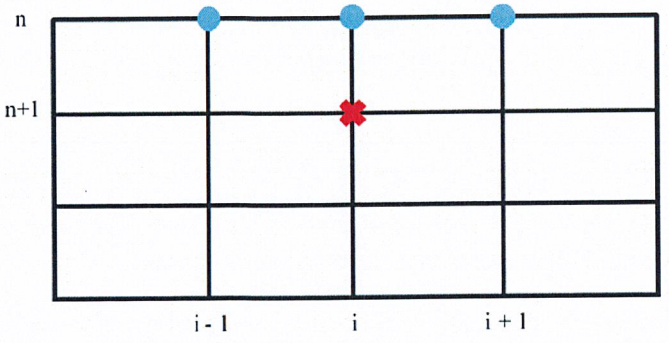

Figure 2.6 Example of an unknown calculation of three upper values, where ● is a known parameter, ✖ is an unknown parameter

2.7 Pressure Drop

Pressure drop is an important parameter that could be used to explanation of aptitude of sizing and forming of the evaporator, it is observed and studied the effects on the rate of evaporation. The evaporator is a type of heat exchanger, [9] shell and tube heat exchanger equations could be adapted to measurement of the pressure drop in shell side of the falling film evaporator. [10] A predictive model is *Bell-Delaware*, in HEDH method the total shell-side pressure drops, there are 3 main parts including ΔP_w is the pressure drop for all baffle windows zone, ΔP_e is the pressure drop for both end zones in the exchanger and ΔP_c is the cross-flow pressure drop for the entire exchanger. The equation of total pressure drop in shell side is

$$\Delta P_{total} = \Delta P_c + \Delta P_{w+} \Delta P_e \tag{2.7.1}$$

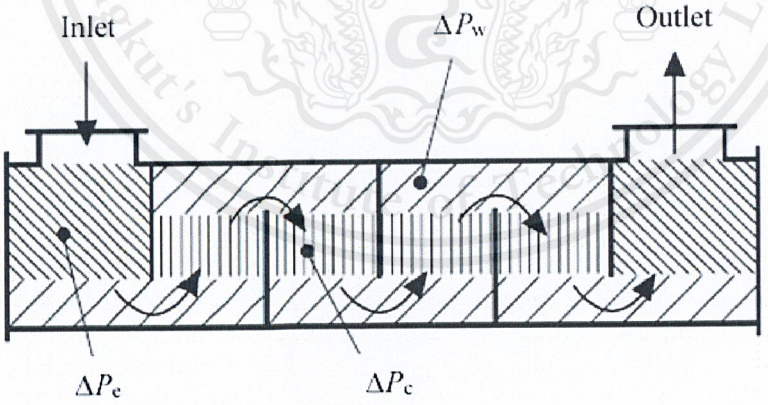

Figure 2.7 Pressure drop calculation parts in shell and tube heat exchanger

For this falling film evaporator, the system with no baffles and only one section is considered, the pressure drops for both end zones and all baffle windows are not mentioned and the pressure drop in shell side for the evaporator contains only the cross-flow pressure drop.

$$\Delta P_{total} = \Delta P_c = \Delta P_{Shell} \tag{2.7.2}$$

The model with a ball-park estimation can be obtained by a relatively simple approach described below [11]

$$\Delta P_{Shell} = \frac{2fG_s^2 D_s (N_B + 1)}{\rho D_e \left(\frac{\mu}{\mu_s}\right)^{0.14}} \tag{2.7.3}$$

In this equation, f is a fanning friction factor for flow on the shell, G_s is the mass velocity on the shell side, D_s is the inside diameter of the shell, N_B is the number of baffles, ρ is the density of the shell-side fluid, and D_e is an equivalent diameter. The mass velocity $G_s = m / S_m$, where m is the mass flow rate of the fluid, and S_m is the crossflow area measured close to the central symmetry plane of the shell containing its axis. This area is defined as

$$\text{Cross flow area} = \gamma D_s L_B \times \frac{\text{clearance}}{\text{pitch}} \tag{2.7.4}$$

Where L_B is the baffle spacing, and the clearance and pitch are defined in the notes on shell-and-tube heat exchangers. The equivalent diameter is defined as follows.

$$D_e = \frac{4\left(C_p S_n^2 - \frac{\pi D_0^2}{4}\right)}{\pi D_0} \tag{2.7.5}$$

Here, γ is summation of the shortest distance between tube center and tube center and tube center and shell surface, D_0 is the outside diameter of the tubes, and S_n is the pitch (center-to-center distance) of the tube assembly. The constant $C_p = 1$ for a square pitch, and $C_p = 0.86$ for a triangular pitch. The friction factor f is given as a function of the Reynolds number based on the equivalent diameter as $f = Re^{-0.15}$, μ is the viscosity of the shell-side fluid and μ_s is the viscosity of the shell-side fluid at the wall surface. A case of incompressible fluid, the viscosity term is sometimes ignored, the changes are small.

$$\text{Re} = \frac{D_e G_s}{\mu} \tag{2.7.6}$$

Rate of evaporation is considered and measured by the overall system containing pitch type, number of tubes, operation pressure and dimension of shell and tube, and pressure drop is reverse proportional to rate of evaporation.

Clearance, pitch and dimension of shell and tube are all relate to the pressure drop directly so, these factors would be varied. γ is less when tubes are closer or too far.

2.8 Heating Media System

2.8.1 The New Design

Because of the new design of falling film evaporator, the heating media system is assembled inside the hot tubes. The micro-level film distributor is very difficult to be possible, the feed film is dropped onto the curve and close tubes. The heating media system is shown in figure 2.8, the upside of tube is slowly flooded as filmy by sugar solution. A sub-tube is inside at the middle of the hot tube to flow direction adjustment of the system.

The counter-counter current flow of the hot water is added at the annulus and it is left at inside of the sub-tube. They are both turbulent flows of the flow entrance and flow exit, heat transfer contained heat conduction in y axis and heat convection in x axis, which is shown in figure 2.9. Temperatures, velocities and heat transfers of the fluid are studied by Fluent program, it is a computational fluid dynamical analysis.

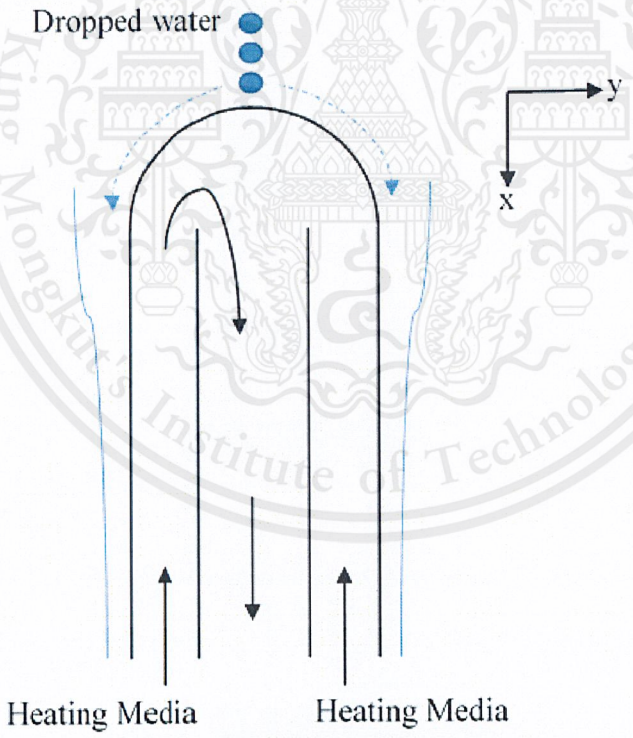

Figure 2.8 Heating media system

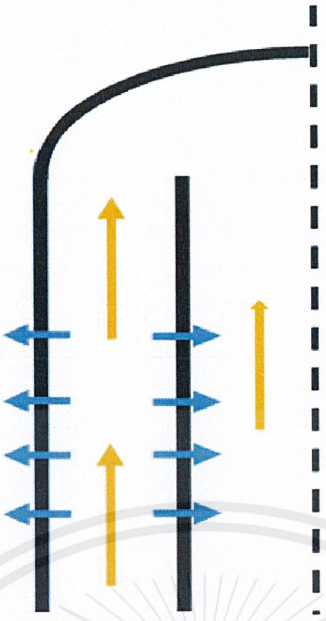

Figure 2.9 Heat transfer in the hot tube, where
and are heat conduction at the wall thickness
are heat convection of hot water

The heat conduction occurs at wall thickness of the hot tube for both left and right sides. The fluid flows with high Reynolds number in range of turbulence, and also heat convection cannot be ignored.

2.8.2 Computational Fluid Dynamics

The computational fluid dynamics (CFD) is a fluid flow analysis that is the use of applied mathematics, physics and software of computation. This numerical method is variously used to engineering calculation, it becomes a commonly applied tools for fluid flows. It is based on the Navier-Stokes equations, the velocity, pressure, temperature and density of moving fluid are described how they are.

This study was set $Y^+ = 30$ because the wall function has been known by heat transfers at the outer wall surface. Then, meshes would be created containing first cell height as follows

$$\Delta y_1 = \frac{Y^+ \mu}{\rho U_T} \tag{2.8.1}$$

Δy_1 is first cell height, μ is viscosity of fluid, ρ is density of fluid and U_T is skin friction velocity. We can define the friction velocity by equation (2.8.2).

$$U_T = \sqrt{\frac{\tau_w}{\rho}} \tag{2.8.2}$$

The shear stress τ_w is equal to $\frac{1}{2} C_f \rho u^2$.

However, this target is to study the movement and heat transfer in the double pipes, an annulus flows and internal flows are concentrated. C_f of internal flows is $0.079Re^{-0.25}$ and u is free steam velocity of fluid.

2.9 Literature Review

Wei et al.[2] studied the presentation on falling film evaporation of water in a vacuum condition. The study was on the 6-row with horizontal enhanced tube bundles, and smooth tubes were tested in a range of film Reynolds number from about 10 to 110. It found the enhanced tube surface provided high effectiveness and better heat transfer performance.

Xianbiao et al.[7] investigated the performance of heat and mass transfer of ammonia water during the process of falling film evaporation in vertical tube evaporator. The mathematical model was provided relations such film velocity, film thickness, and concentration, etc.. The calculated results showed the film velocity and thickness sharply changed at the entrance region.

Alberto et al.[12] simulated a model involved the falling film evaporator, this was based on Nusselt falling film theory and Newton's viscosity law. The model was clearly demonstrated for a good performance in air-conditioning and refrigeration of falling film evaporators. And this study also investigated advantages of each vary tube models.

Roman et al.[13] studied heat transfer to evaporating liquid films within a vertical tube. The evaporating of saturated liquid film of isopropanol, methanol, and water inside a vertical tube with low to high heat fluxes. This study investigated the range of high heat fluxes could be considered with a boiling number if nucleate boiling was developed, it could be shown the upper limit of convective heat flow.

Chuang et al.[14] studied factors which affect falling film evaporation coefficients in a horizontal enhanced tube bundle using R134a. The results indicated that the film flow rate, heat flux, saturated temperature all have significant effects on the falling film evaporation. The film flow rate decreases, the local and average heat transfer coefficients are taken a tendency of firstly sharp increasing and then rapid decreasing. And the performance is proportional to an increase in saturated temperature but worse with heat flux.

Fengzhen et al.[15] had designed a new header configuration with perforated baffle plate, that can decrease the middle speed then more uniform distributions appear. This numerical simulation aimed to characterize the optimum design of distributor. That can improve the higher speed refrigerant (or heat transfer medium) near the inlet of distributors.

CHAPTER III
RESEARCH METHODOLOGY

3.1 The Developed Model

The old model was designed and studied by almost steps followed chapter 3.3.1. It was provided the useful data to know disadvantages of the evaporation system, the concentration of the falling film was increased only 20-30% from the film surface the inside one was got no changes or very small changes in concentration. The study was found that the outlet concentrated sugar solution was 23.25 wt% from 15 wt%. The method of improvement was adding an equipment called collector at the middle of the hot tube that would be varied 2 types: 1.) make the well-mixed sugar solution 2.) lead the inner film layer to the film surface before the next half evaporation. These could be raised the concentrated product up by small values.

The current model aims to eliminate limitations from the assumptions, which it leads to more real system and more overall system consideration such as

- Inconstant of sugar solution properties
- Tubes distribution
- Parameters that effect on pressure drop
- How to produce more concentrated sugar solution
- Optimization

3.2 Calculation and Analysis Tools

1. MATLAB R2017a
2. Microsoft Excel 2016
3. GAMBIT 2.4.6
4. FLUENT 19.0

3.3 Procedure

3.3.1 Film Calculation Steps

Since there are a lot of variables involving the iterative calculations, some of these are firstly assumed and they would be rechecked later. The first row (n = 1) is the feed layer, that means we take the conditions for row n = 1 as the feed and start the iterations at row n = 2. Reynolds number, a dimension of the tube, properties of heating media and size of gridlines are fixed for a set of the calculation.

For this project, the initial conditions for the simplest model are described by

- Feed starts at row n = 1.
- Column i = 1, film temperature is equal to tube wall temperature.
- Column i = 1, no changes in film concentration appear.

The brief steps are shown as follows

1. Assume tube wall temperature
2. Assume evaporated mass flux
3. Calculate film thickness and film flow rate (Chapter 2.2.2)
4. Calculate film velocity (Chapter 2.2.2)
5. Calculate the coefficient variables in equations (2.6.7) and (2.6.8)
6. Use the values from step 5. determining the film concentration and temperature
7. Calculate the film surface concentration by equations (2.3.2) and (2.3.3), then it can be defined the film surface temperature by Antoine equation (2.4.2)
8. Recheck evaporated mass flux by equation (2.4.1). Do the next step if the rechecked value is acceptable, but if not the step 2 would be repeated
9. Rechecked tube wall temperature by relationship (2.3.1). Do the next step if the rechecked value is acceptable, but if not the step 1 would be repeated
10. Completely finish calculation for that row and keep repeating for the next row

These steps would be rewritten in a flowchart to easier overview. The steps have been finished and provided the concentration and temperature profiles of falling film during the process of evaporation occurred meanwhile.

Flowchart

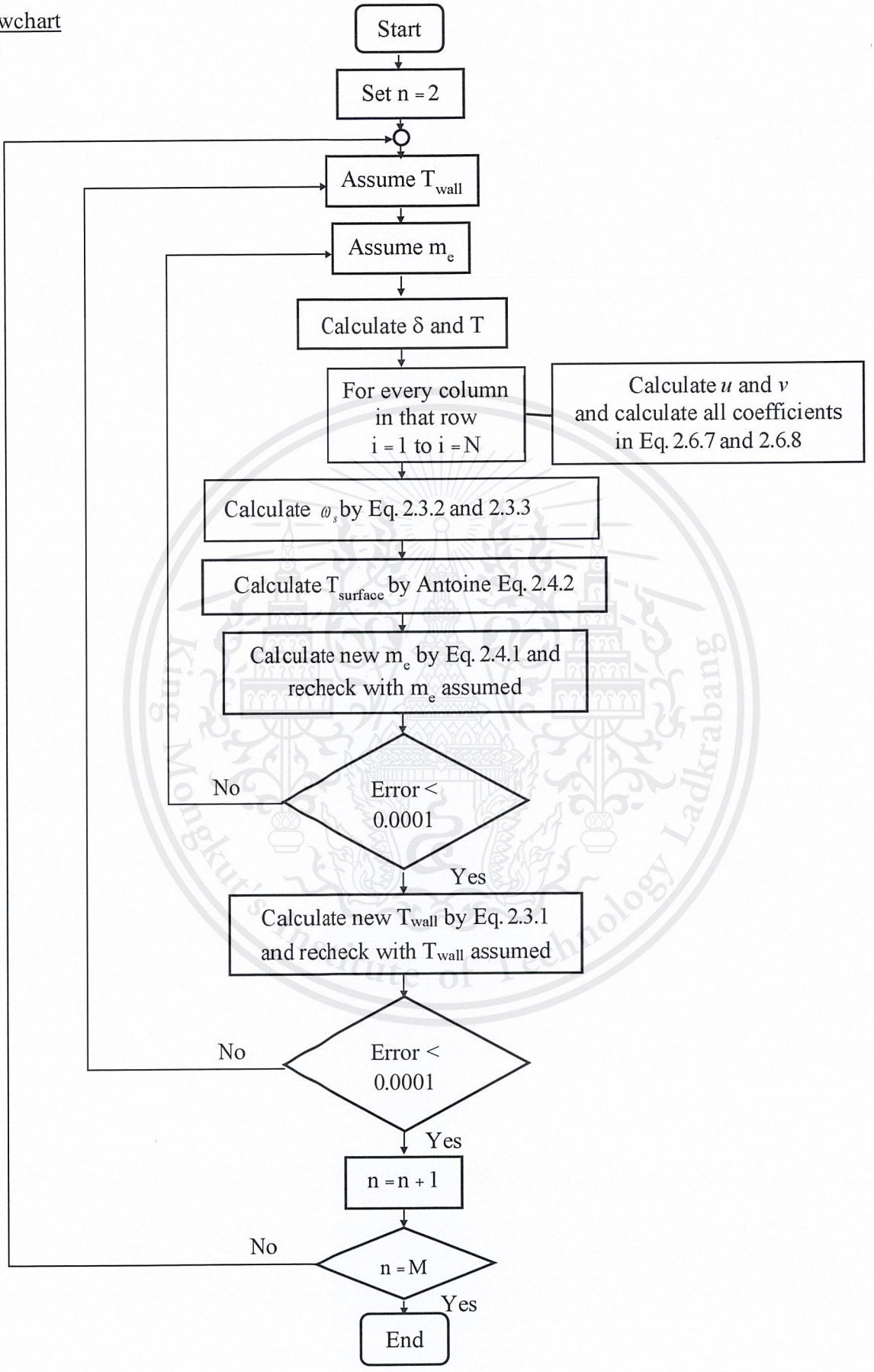

3.3.2 Pressure Drop in Shell Side

The pressure drop is calculated via MATLAB R2017a by the details in chapter 2.7.

Independent variables

1. Pressure (40, 50 and 60 mmHg)
2. Shell diameter (8, 10, 12 and 15 inch)
3. Tube diameter (3/4, 1, 5/4, 3/2 and 2 inch)
4. Pitch type (triangular pitch and square pitch)
5. Distribution of tubes (vary k = 0.90, 0.95, 1.00, 1.05 and 1.10)

Dependent variables

1. Pressure drop
2. Rate of evaporation
3. Energy efficiency

We firstly study the effects of tubes distribution because it depends on shell and tube diameter and pitch type. The case of 40 mmHg of pressure, shell and tube are 10 and 2 inches of diameter and triangular pitch type is fixed to study the pressure drop in shell side of changes in distribution of tubes. Then, we would take the relationship of distance of tube to tube and tube to shell.

3.3.3 Heating Media System

Independent variables

1. Inlet velocity of hot water depended on design (0.1984 and 0.2858 m/s)
2. Materials of tube (stainless steel 304 and stainless steel 430)
3. Head radius of the tube, radius of tube is R (R and R/2)

Dependent variables

1. Outlet temperature
2. Temperature difference

This step is taken after we design the overall system from chapter 3.3.1 and 3.3.2. The hot fluid is studied by a computational fluid dynamics (CFD), the study tools are 2 parts, GAMBIT 2.4.6 and FLUENT 19.0.

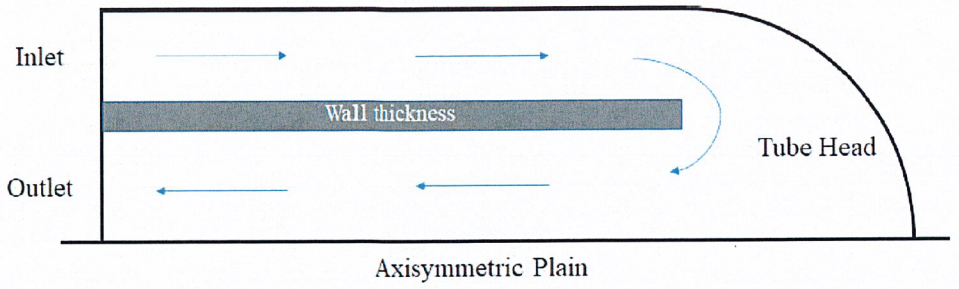

Figure 3.1 The mesh design creation in GAMBIT

GAMBIT 2.4.6

1. Calculate Δy_1 for each case, including inlet flow part and outlet flow part
2. Draw meshes following the required design in 2 dimension

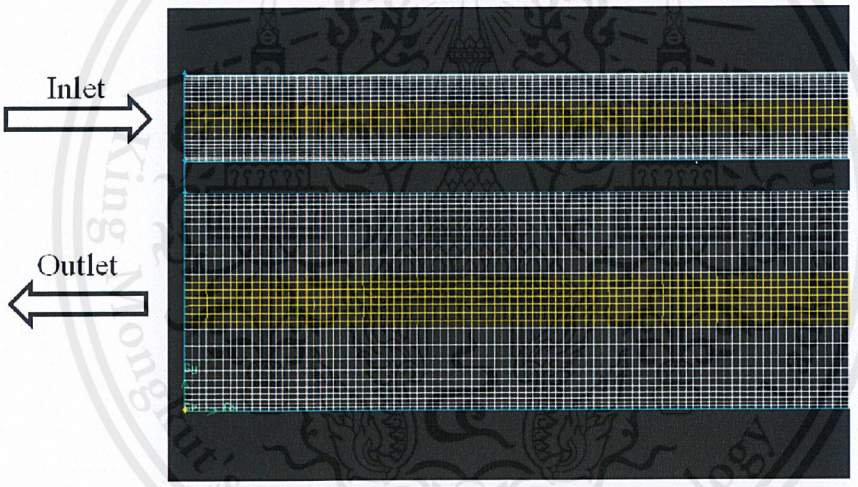

Figure 3.2 Inlet and outlet parts of mesh design 1

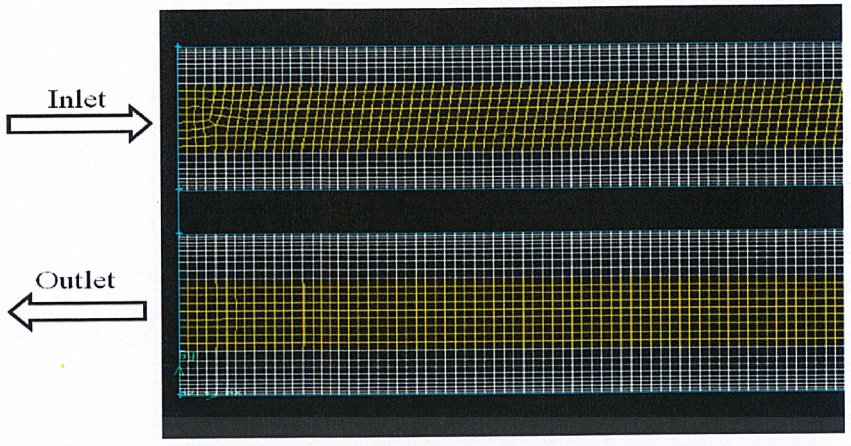

Figure 3.3 Inlet and outlet parts of mesh design 2

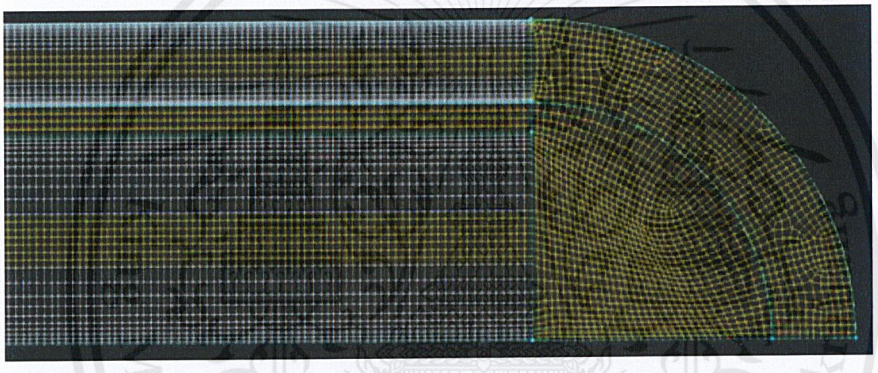

Figure 3.4 Example of tube head part

Note Figure 3.2 and 3.3 show examples of the meshes at the inlet and outlet zone, the white zone is 1.2 of the growth rate and the yellow zone is constant growth rate with 0.5 of interval spacing. GAMBIT and FLUENT are set the fluid flow direction in x-axis, the created meshes appeared based on horizontal tubes.

3. Set the fluid and solid region following the boundary conditions

    3.1 Set the entrance flow to Velocity_Inlet

    3.2 Set the exit flow to Pressure_Outlet

4. Export to a mesh file

FLUENT 19.0

1. Import the mesh file
2. Set up
    2.1 Go to General
        2.1.1 Adjust scale
        2.1.2 Set 2D space to axisymmetric
        2.1.3 Set gravity
    2.2 Go to Models
        2.2.1 Change Energy to mode on
        2.2.2 Change Viscous (laminar) to k-epsilon
    2.3 Go to Materials
        2.3.1 Add water liquid to Fluent database in fluid
        2.3.2 Add steel to Fluent database in solid (manual property addition)
    2.4 Go to boundary conditions and set all boundary conditions
3. Solution
    3.1 Go to Methods
        3.3.1 Set turbulent kinetic energy to second order upwind
        3.3.2 Set turbulent dissipation rate to second order upwind
    3.2 Go to Residual and uncheck all the monitor check convergence absolute criteria in the right hand side
    3.3 Go to Calculation activities and Run calculation
4. Check the outlet velocity and temperature in the results

CHAPTER IV
RESULTS AND DISCUSSION

4.1 Film Calculations

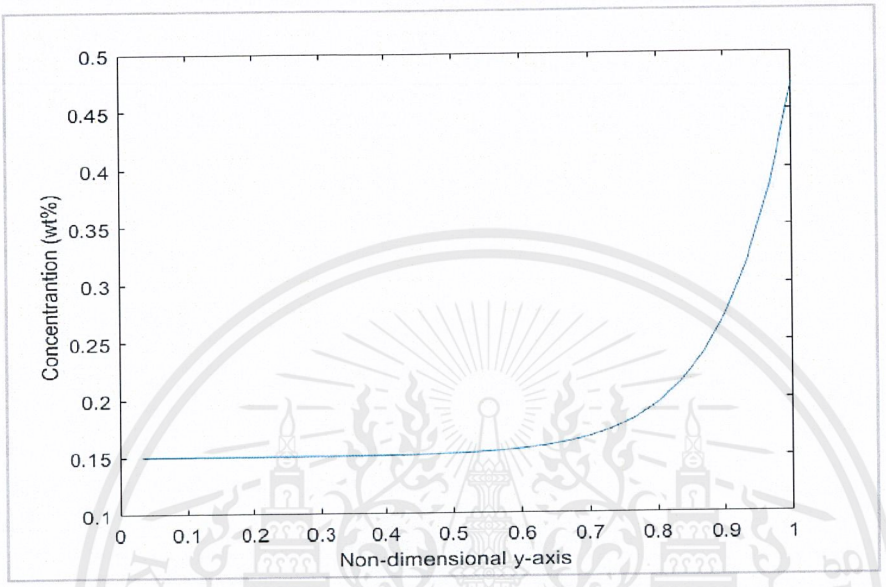

Figure 4.1 Average film concentration of non-dimensional y-axis direction

The evaporation of the film appeared only 20-30 % from the film surface, it caused high concentration at the surface but other zones was almost constant at 15 wt%. We used MATLAB to calculate the characteristic of the film involving the temperature profile and concentration profile. The film was fixed the flow by Reynolds number and tube diameter, and we considered at Re = 150 which is the range of laminar flow with acceptable pronounced rippling.

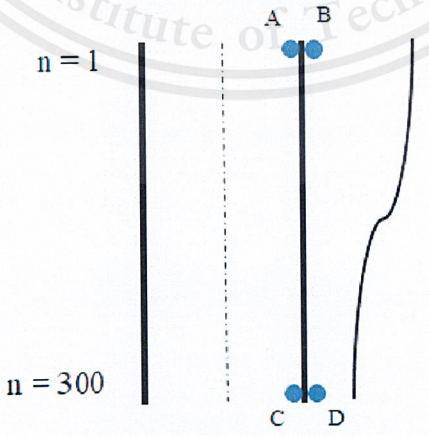

Figure 4.2 Temperature differences at heating wall thickness

A and C represent to temperature of inner tube at the first and last row.

B and D represent to temperature of outer tube at the first and last row.

Table 1 Temperature at the first row n = 1 and the last row n = 300

Material	A (°C)	B (°C)	C (°C)	D (°C)
Stainless steel 304	62.7	59.1	75.6	70.0
Stainless steel 430	61.2	59.1	73.4	70.0

This point aimed to consider heat conduction at the wall thickness between the hot water and the falling film. The points B and D were fixed by the calculation in chapter 2.3, if the point A and C much differed from B and D, the heat conduction was not effective because the system required high heat duty. Stainless steel 403 was better than stainless steel 304, its thermal conductivity is higher and heat duty is less.

4.2 Pressure Drop in Shell Side

The distribution of tubes was firstly observed by fixed the other parameters. The case of 40 mmHg of operated pressure, shell and tube are 10 and 2 inches of diameter and triangular pitch type was considered.

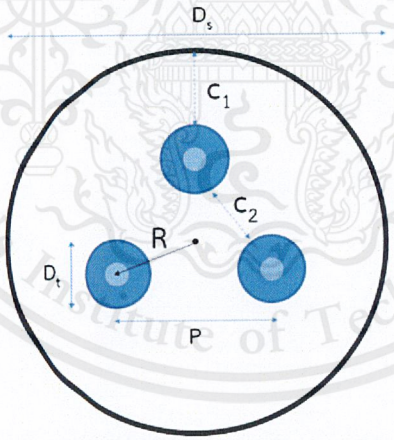

Figure 4.3 Top view of the cross section of tube

The figure 4.3 shows the furthermost distance from tube to tube and tube to shell related as following equation for square pitch type.

$$P = \frac{3}{2}\frac{(D_s + D_t)}{(\sqrt{3} + 3)} \qquad (4.2.1)$$

Hence, P is pitch (tube center to tube center), C is clearance (tube surface to tube surface), D_s is shell diameter and D_t is tube diameter. Distance from the center of shell and center of tube is radius R, which $R = P/\sqrt{3}$.

The calculation was planned by changes of the distance from the center of shell and center of tube in term of r = kR, where k is constant value.

Table 2 Effects of tubes distribution variations on pressure drop in shell side for the case of 40 mmHg of pressure, shell and tube are 10 and 2 inches of diameter and triangular pitch type design

k	0.90	0.95	1.00	1.05	1.10
Pressure drop (mmHg)	1.6704	1.418	1.2167	1.3322	1.5622

The pressure drop in shell side was decreased when addition of k value, when k = 1 the pressure drop in shell side was increased continuously. The results show that the pressure drop in shell side of the case with R is equal to 1 time of R is the least respect to the others. Therefore, we chose the pitch of square pitch type from 1 time of pitch in equation (4.1) and in the same way of the triangular pitch type, its pitch was measured by equation (4.2).

$$P = \frac{(D_s + D_t)}{(\sqrt{2} + 2)} \qquad (4.2.2)$$

Where, $R = P/\sqrt{2}$

The cross flow area is the parameter containing the factor γ that takes the maximum value while the tubes are distributed properly (r = R or k =1). The lower k value would get the closer distance of tubes, the cross flow area of the tubes was not effective. However, the too high k value, the tube and shell is closer. The distances between surface to surface lead to efficiency of fluid flow, especially higher viscous fluids because viscosity or density of the fluids involve with shear stress.

Next step was fixing this result that was using the pitch in equation (4.1) and (4.2) for measurement and studying the others parameter. The tube and shell diameters were varied, pressure drop, rate of evaporation and energy efficiency were observed. The results are shown as follows

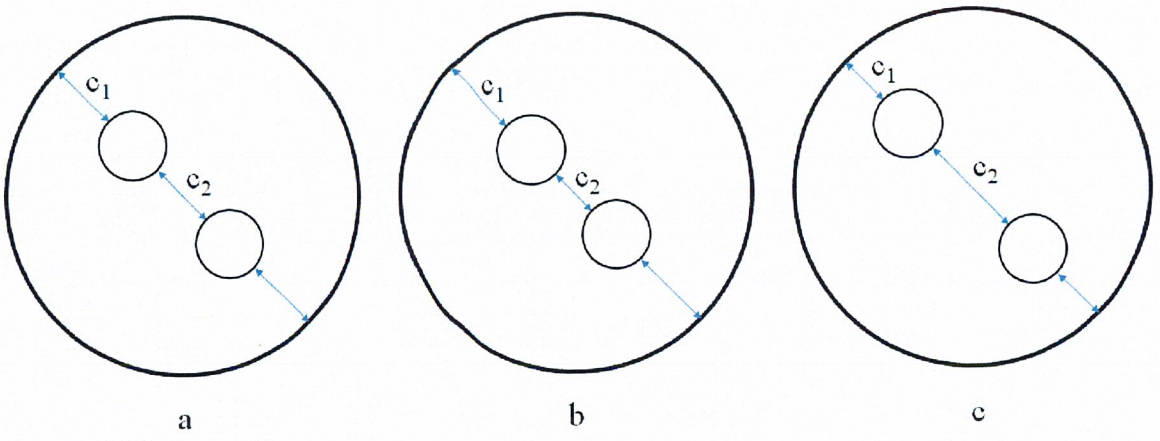

Figure 4.4 Distance from tube to tube and distance from shell to shell

a. $c_1 = c_2$ and $k = 1$

b. $c_1 > c_2$ and $k < 1$

c. $c_1 < c_2$ and $k > 1$

k is a parameter assumed to taking the various designs of the tube distribution. When k is less than 1, the distance between tube and tube is closer, and k is higher, the distance between tube and shell is closer.

For 40 mmHg

Pressure drop

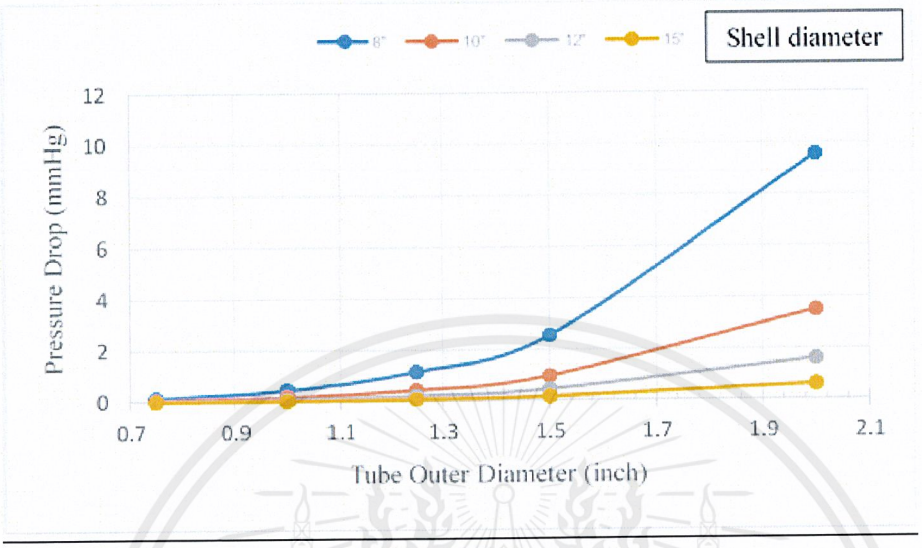

Figure 4.5 Effect of shell and tube diameter variation on pressure drop for square pitch design at 40 mmHg

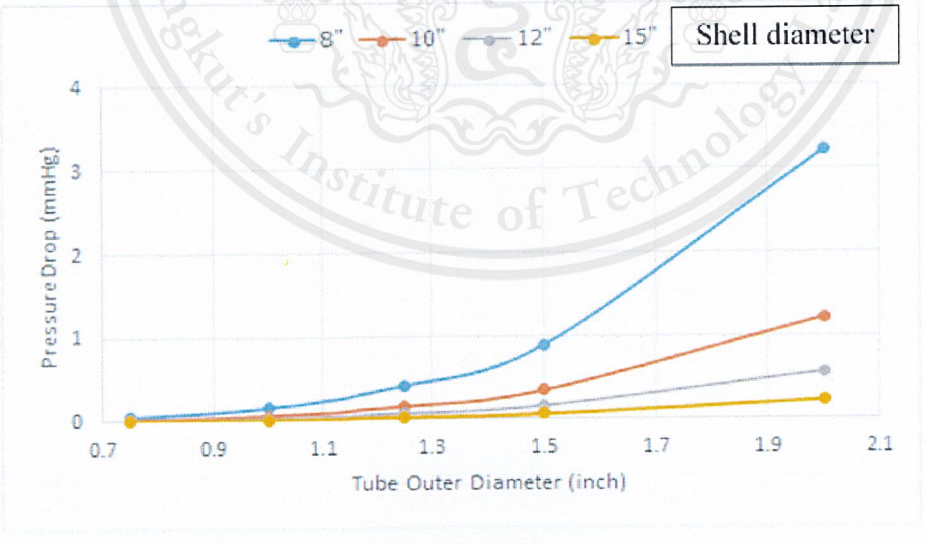

Figure 4.6 Effect of shell and tube diameter variation on pressure drop for triangular pitch design at 40 mmHg

Rate of evaporation

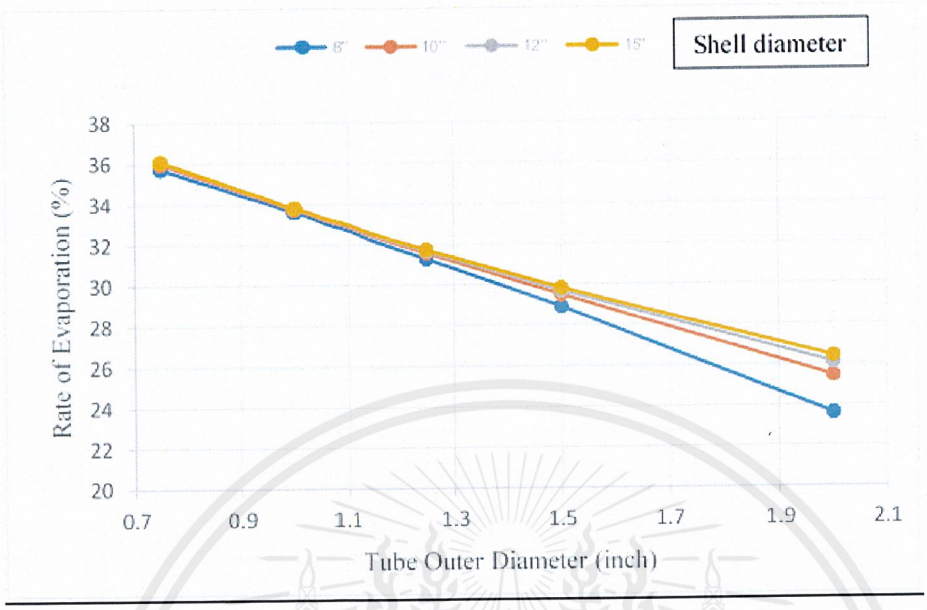

Figure 4.7 Effect of shell and tube diameter variation on rate of evaporation for square pitch design at 40 mmHg

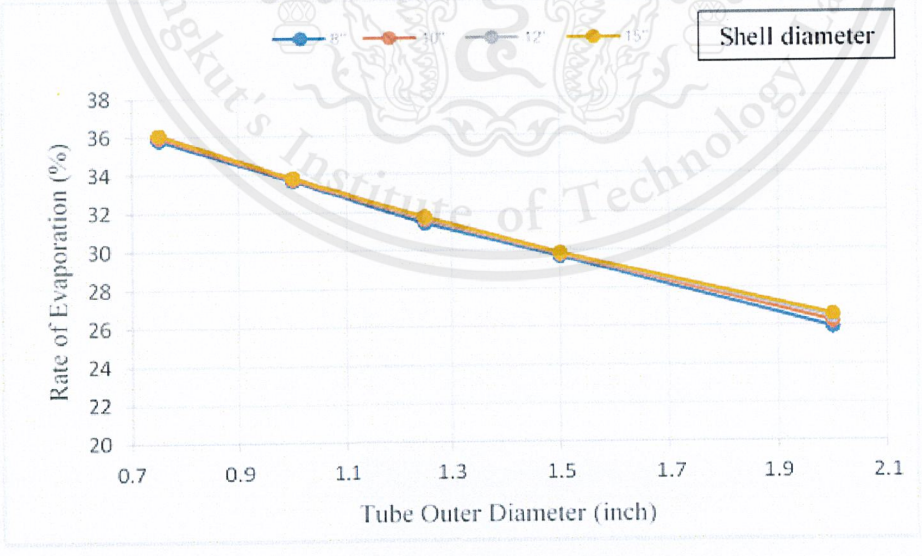

Figure 4.8 Effect of shell and tube diameter variation on rate of evaporation for triangular pitch design at 40 mmHg

Energy efficiency

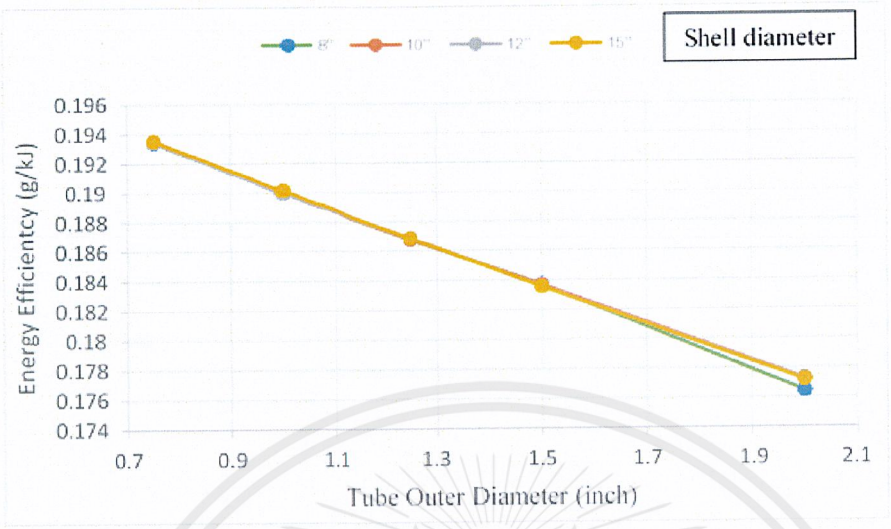

Figure 4.9 Effect of shell and tube diameter variation on energy efficiency for square pitch design at 40 mmHg

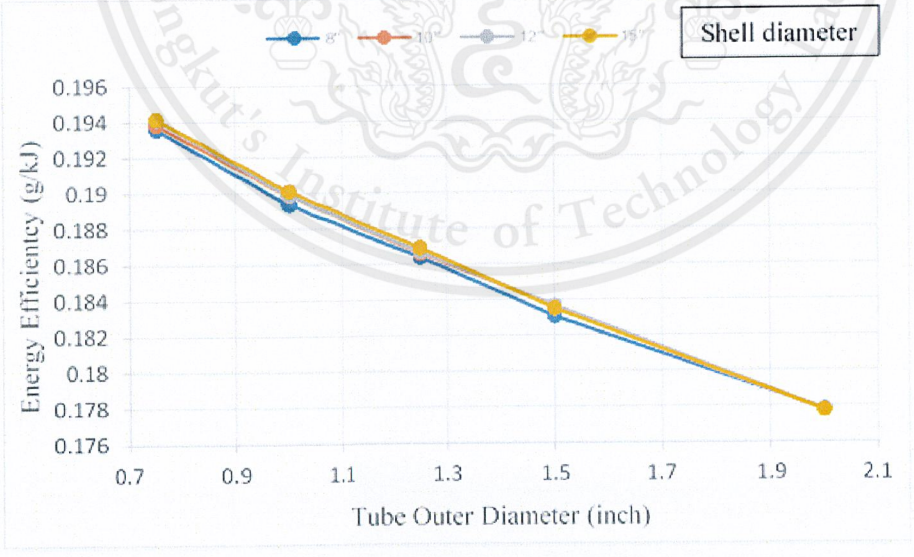

Figure 4.10 Effect of shell and tube diameter variation on energy efficiency for triangular pitch design at 40 mmHg

For 50 mmHg

Pressure drop

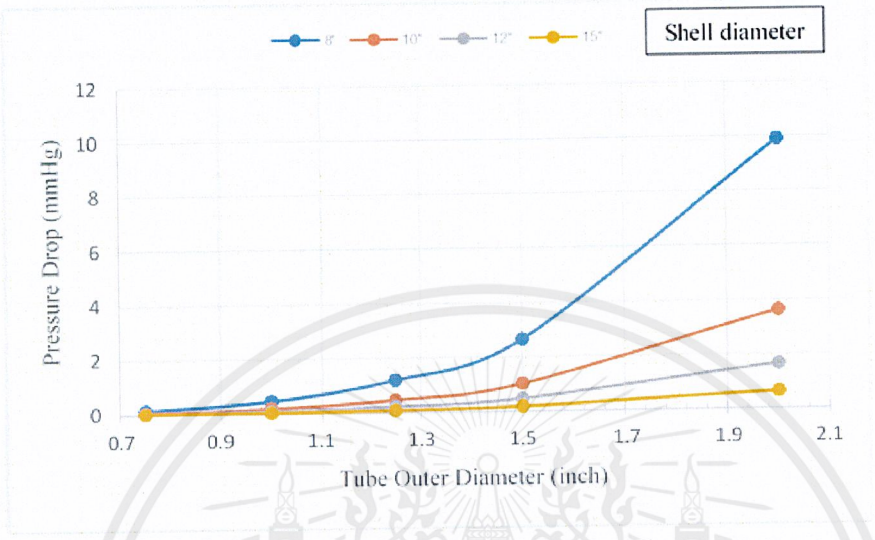

Figure 4.11 Effect of shell and tube diameter variation on pressure drop for square pitch design at 50 mmHg

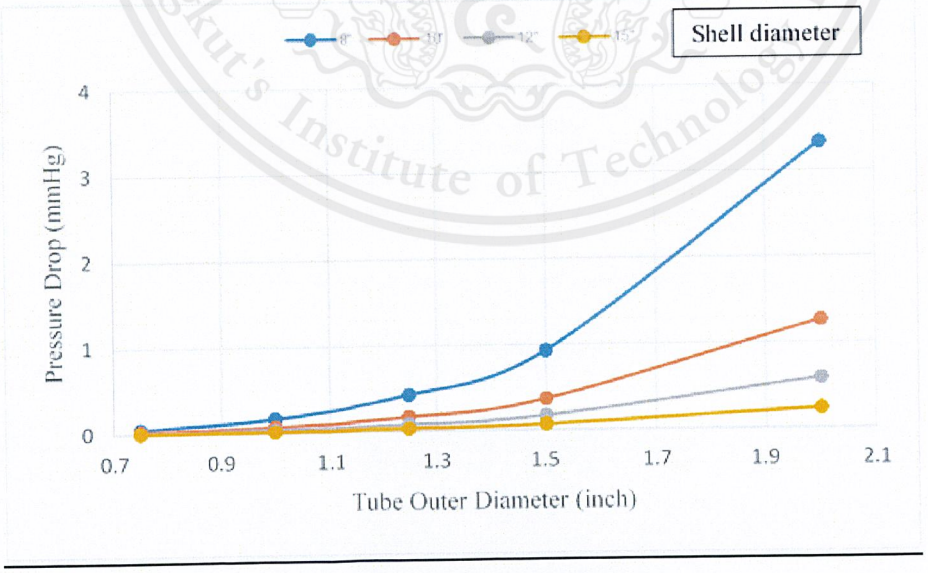

Figure 4.12 Effect of shell and tube diameter variation on pressure drop for triangular pitch design at 50 mmHg

Rate of evaporation

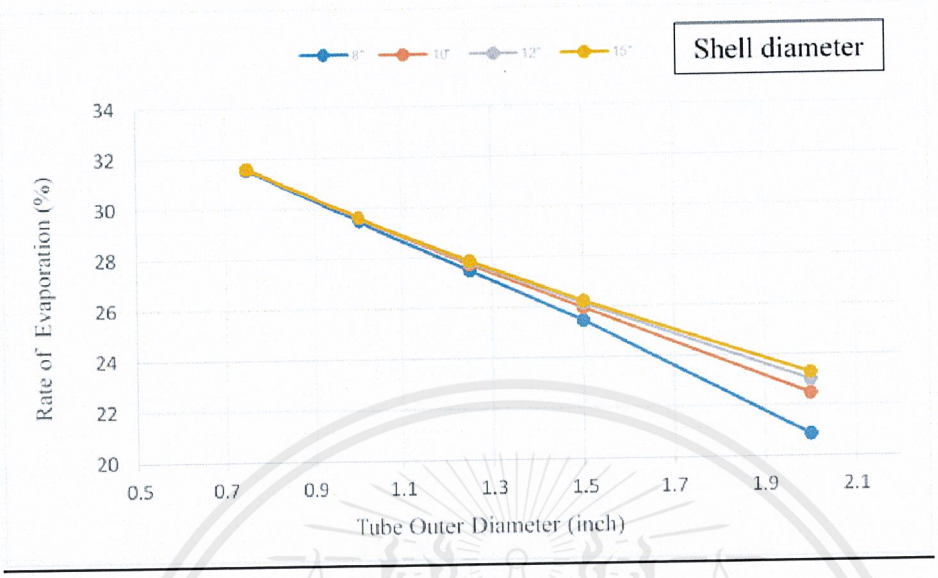

Figure 4.13 Effect of shell and tube diameter variation on rate of evaporation for square pitch design at 50 mmHg

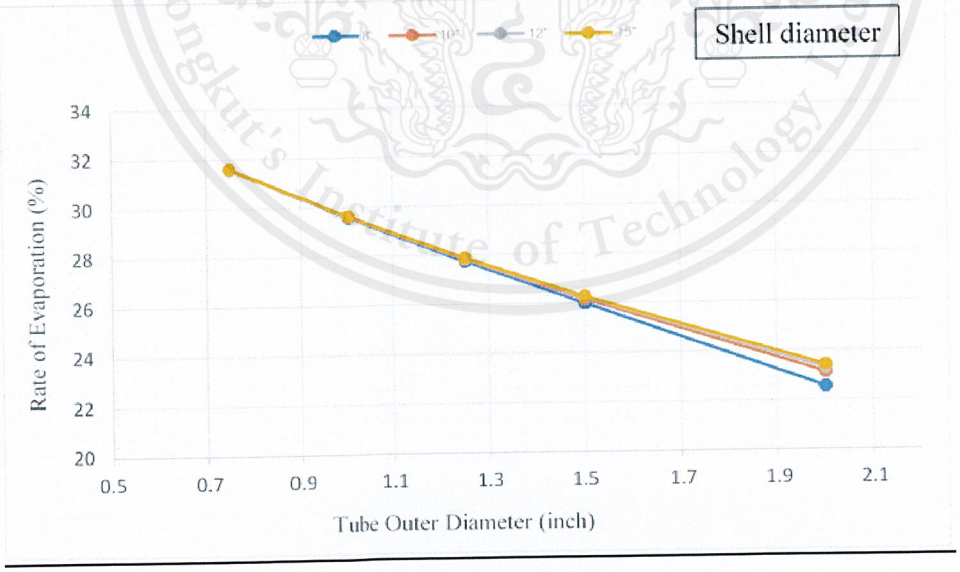

Figure 4.14 Effect of shell and tube diameter variation on rate of evaporation for triangular pitch design at 50 mmHg

Energy efficiency

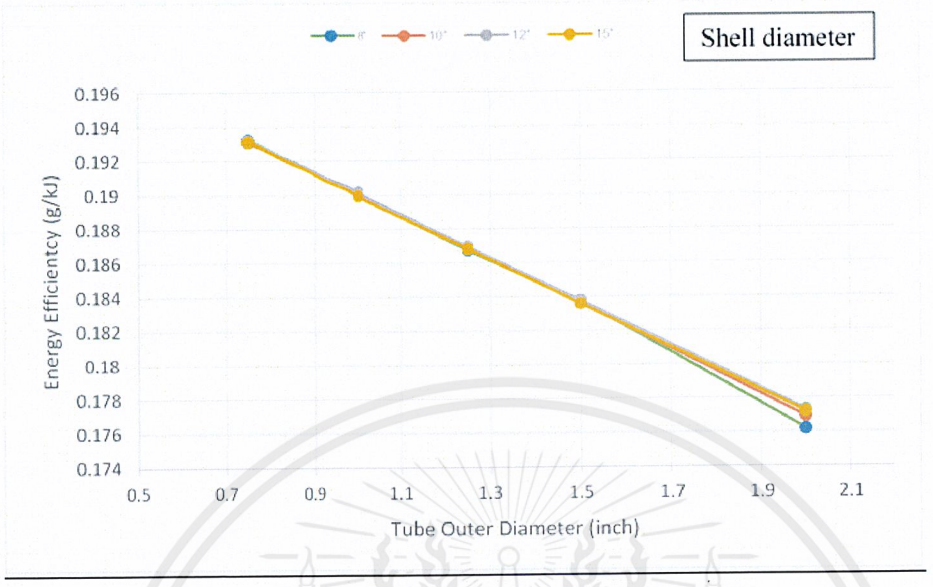

Figure 4.15 Effect of shell and tube diameter variation on energy efficiency for square pitch design at 50 mmHg

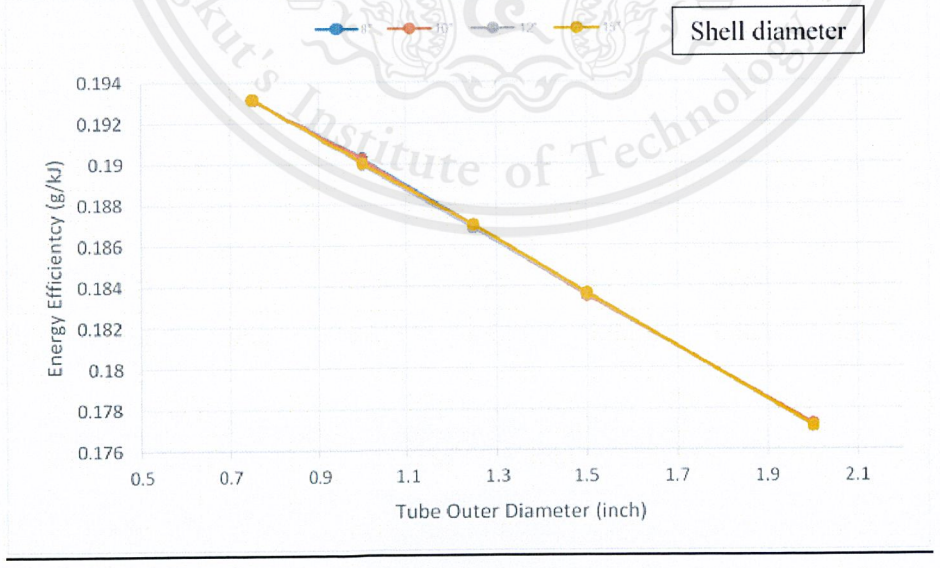

Figure 4.16 Effect of shell and tube diameter variation on energy efficiency for triangular pitch design at 50 mmHg

For 60 mmHg

Pressure drop

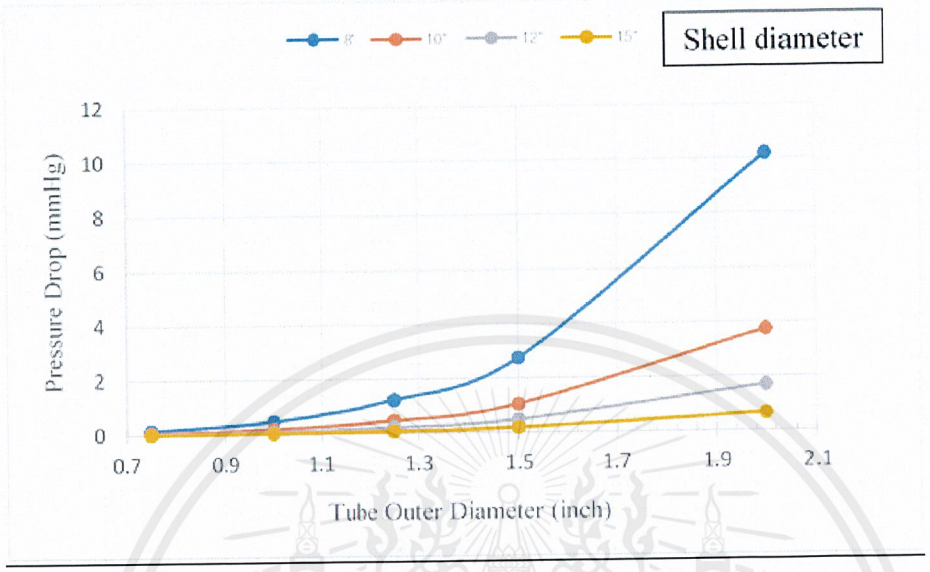

Figure 4.17 Effect of shell and tube diameter variation on pressure drop for square pitch design at 60 mmHg

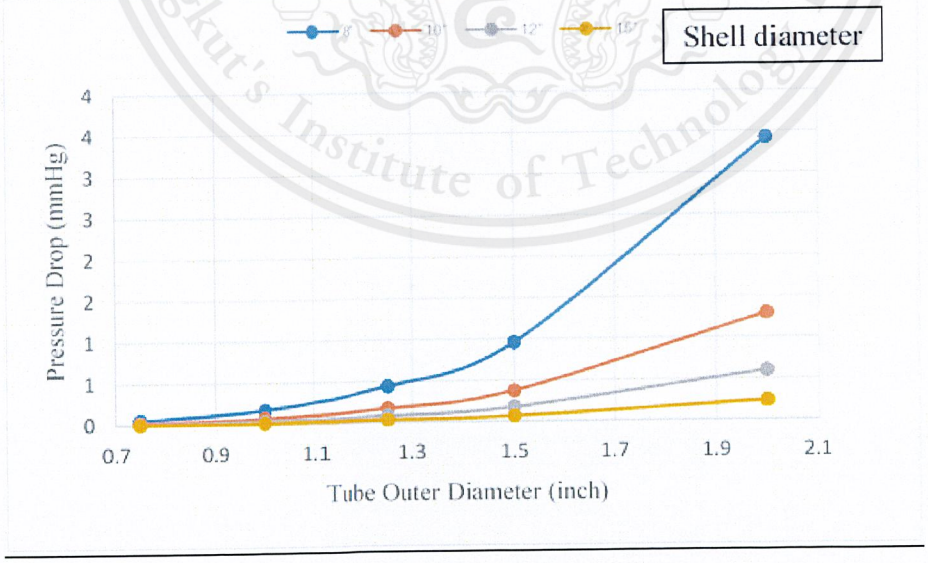

Figure 4. Effect of shell and tube diameter variation on pressure drop for triangular pitch design at 60 mmHg

Rate of evaporation

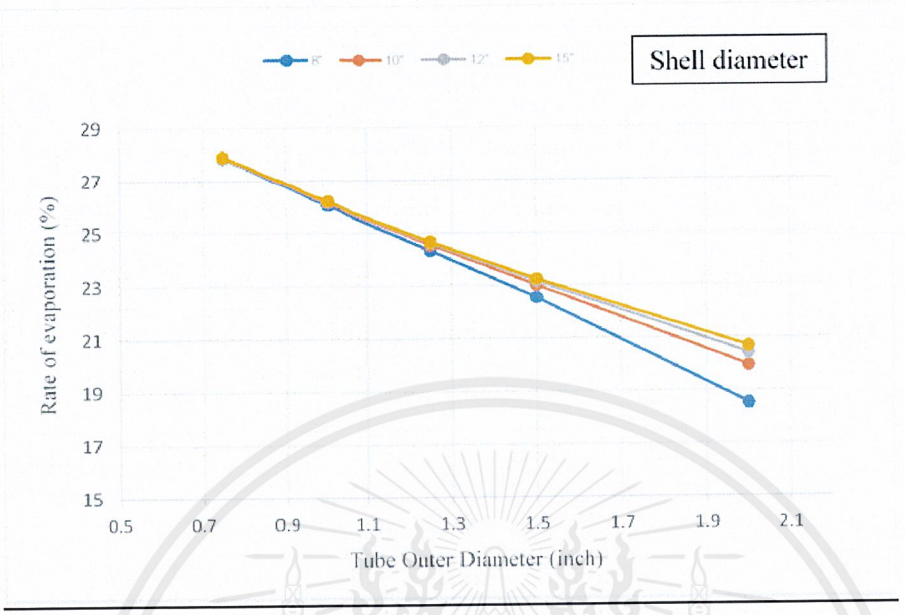

Figure 4.19 Effect of shell and tube diameter variation on rate of evaporation for square pitch design at 60 mmHg

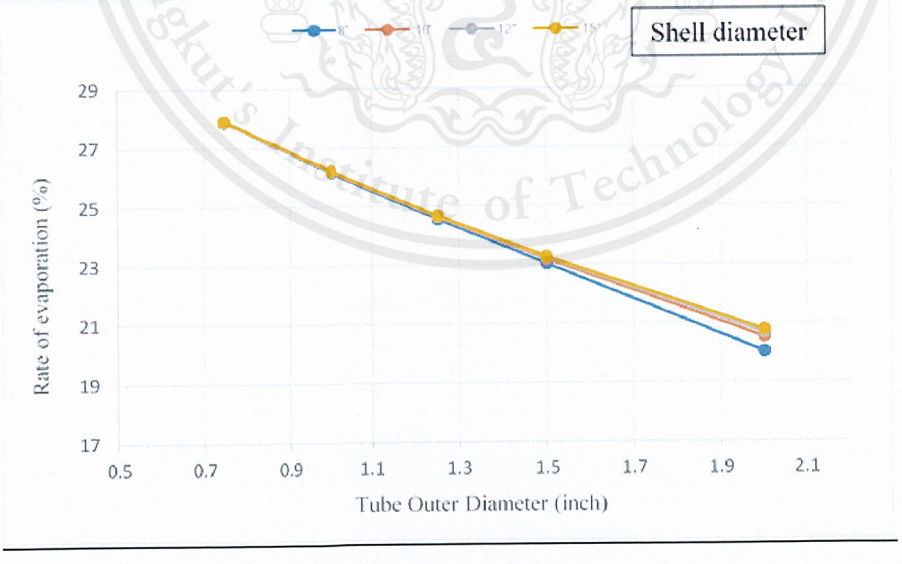

Figure 4.20 Effect of shell and tube diameter variation on rate of evaporation for triangular pitch design at 60 mmHg

Energy efficiency

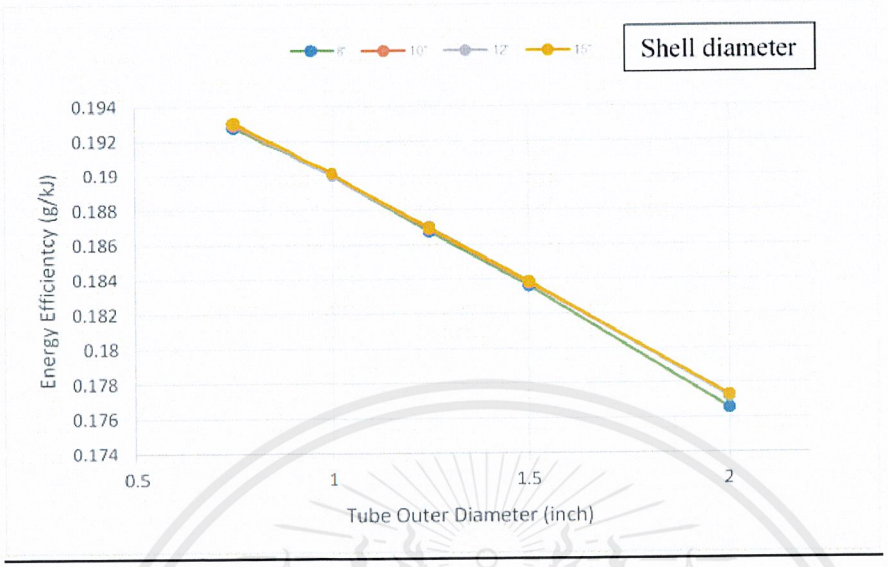

Figure 4.21 Effect of shell and tube diameter variation on energy efficiency for square pitch design at 60 mmHg

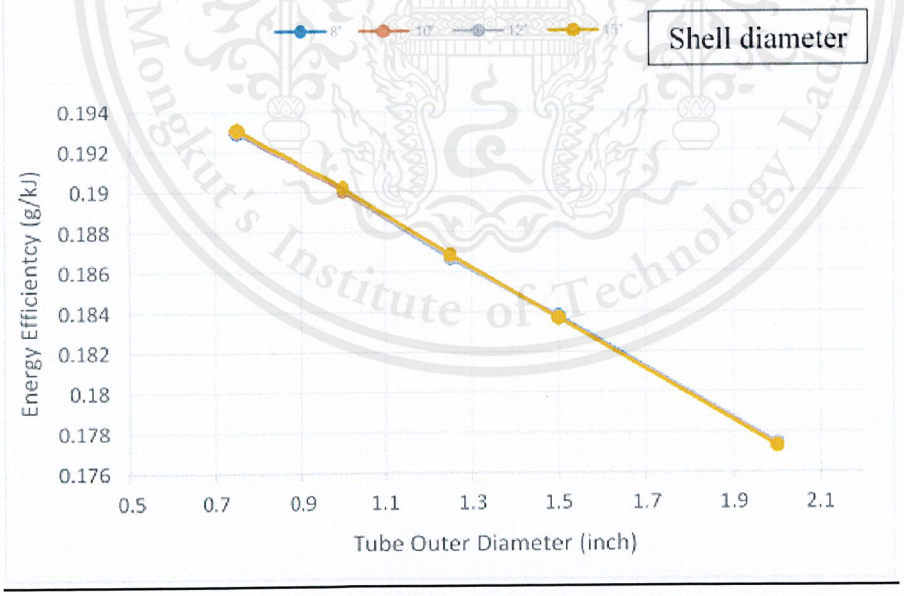

Figure 4.22 Effect of shell and tube diameter variation on evaporation for triangular pitch design at 60 mmHg

The shell and tube diameters are all assumed in a proper ranges (the tube schedules are maybe not exist).

The main concentrated outputs were rate of evaporation and pressure drop. Firstly, we checked the relation graphs and analyzed the dissimilar cases. The energy efficiency could be used to optimization of energy consummation and rate of evaporation. We recalled that feed is 15 wt% of sugar solution, it would be evaporated and produced over 20 wt% of concentration. The variations of shell and tube sizes mean the amount of feeds is depended on its tube dimension, the feed film falls down being cover the outer hot tube surface. The number of tube follows the types of pitch, so changing a parameter may affects some other parameters instantaneously.

For 40 mmHg case, rates of evaporation of triangular pitch type are mostly similar, the only case of 8-ince shell and 2-inch tube design looks different, but it is little dissimilar. That means pressure drop around 3.2 mmHg affects to the rate of evaporation little, if we say that the other cases is full efficiency of evaporation, 3.2 mmHg of pressure drop will drop around 0.5 % of rate of evaporation. Considering to square pitch type, some results are clearly different, especially the case of 8-inch shell. This case generally takes higher pressure drop and is surely decreased the rate of evaporation, it is the smallest shell diameter. We will check the cases that take more pressure drop than around 3.2 mmHg. The case 10-inch shell with 2-inch tube can be discussed as the case of 8-ince shell and 2-inch because rate of evaporation is not still much different, 3.5 mmHg causes around 1% decreasing of rate of evaporation. The square pitch could be used clearly to study the effects of higher pressure drop, pressure drop range is more than triangular pitch than 3 times of its. It causes the rates of evaporation are dropped. We skipped to consider the case of 8-inch shell and 2-inch tube for square pitch type design. The pressure drop at 9.5 mmHg of this case shows that it starts a greater effect around 2.5%. This first case (40 mmHg) concludes the great pressure drop effect will be over 3.5 mmHg with 1% rate of evaporation dropping. The energy efficiency would be considered later or optimization part approaches.

For 50 mmHg case and 60 mmHg case, they were considered as 40 mmHg case similarly. Their systems took higher pressure drop than the last case, and 60 mmHg case is the highest for each. However, the pressure drop for 3 cases are not significantly different, which look like the same relations. Increasing the operated pressure (10 mmHg) reduced its rate of evaporation in wide range. The operated pressure is the one main important condition of this calculation, higher pressure causes the boiling point of water is higher too, but the system could not change the inlet temperature of hot water, we basically fixed this condition to study the characteristics of film in terms of temperature and concentration. Heat duty for higher operated pressure increased while energy input was constant, so the rate of evaporation was decreased numerously.

In part of selecting criteria, product should be higher than 20 wt% or taking equivalent or over 25% of rate of evaporation, the tube size is not too small because it would be packed inside by the smaller sub-tube for the heating media system and the energy requirement is properly acceptable. Considering 60 mmHg case, the functional cases were all contained by the small tubes for both triangular and square pitch type (3/4-inch and 1-inch tube), we thought

that they were too small to be choices. Comparing between 40 mmHg and 50 mmHg case, they could be almost selected except the smallest shell side (8-inch shell). Bigger shell sizes were surely taken lower pressure drop in shell side, it was likewise more expensive however, the 8-inch shell was considered.

Table 3 Rate of evaporation of 40 and 50 mmHg of operated pressure

Parameter	Pressure	Triangular pitch type					Square pitch type				
		Diameter of tube (inch)					Diameter of tube (inch)				
		3/4	1	5/4	3/2	2	3/4	1	5/4	3/2	2
Rate of evaporation (%)	40 mmHg	35.8	33.7	31.4	29.7	25.9	35.7	33.6	31.2	28.9	23.6
	50 mmHg	31.6	29.6	27.8	26.0	22.5	31.5	29.4	27.5	25.4	20.9

The double-under lines shown the non-functional results which the rates of evaporation were under 25%. Interesting cases were shown with the single-under lines. The system was more than is necessary reduced the pressure to 40 mmHg for production of 20 wt% sugar solution, and square pitch type could be used to product higher product. Therefore, the case of 8-inch shell and 3/2-inch tube design distributed with square pitch type and operated at 50 mmHg.

The actual schedules were considered and the sizes selection is shown in table 4

Table 4 Actual shell and tube size

	Shell (inch)		Tube (inch)	
Diameter (inch)	OD	ID	OD	ID
	8.625	8.071	1.9	1.774
Wall thickness (inch)	0.277		0.065	
Diameter (m)	OD	ID	OD	ID
	0.2191	0.0250	0.0483	0.0451
Wall thickness (m)	0.007		0.0017	

Finally, the actual schedule makes the pressure drop in shell side as 4.9882 mmHg and 25.0876% of rate of evaporation.

4.3 Heating Media System

The 8 cases were studied by FLUENT program, each of them were required for different purposes. Different materials were studied the differences of heat transfer efficiency. Different designs were studied the differences of fluid velocity. The varied inlet velocity depended on its design, the inlet velocity of case 1 was 0.2858 m/s and another case is 0.1984 m/s.

The designed meshes were created by GAMBIT program, the first cell height is important for fluid flow numerical method as computational fluid dynamics, especially turbulent flow in pipes. The basic was using to creating the meshes, growth rate is 1.2 constant. Changings in viscosity and density of incompressible fluid were negligible. High value of first cell height means density of that mesh is loose, it is not necessary to be a dense grids. As the design 2, it is different obviously for inlet and outlet part.

Differences of inlet and outlet velocity are study by the design 1 and design 2, another objective is how differences of heat transfer are. The first cell height could lead more accuracy because the turbulent flows are difficultly studied.

The 2 designs were calculated and created, the basic first cell height is shown in Table4.

Table 5 Data of the first cell height calculation

Design	Part	U (m/s)	$D_H x10^2$ (m)	Re (-)	$C_f x10^3$ (-)	τ_w (Pa.s)	$U_T x10^4$ (m/s)	$\Delta y_1 x10^5$ (m)
1	Inlet	0.2858	1.166	8866	8.14	0.3231	1.7	7
	Outlet	0.3368	1.459	13078	7.39	0.4071	2.1	5
2	Inlet	0.1984	1.839	9708	7.96	0.1522	0.8	14
	Outlet	0.6448	1.046	17955	6.82	0.1378	7.1	2

The first cell height was used to create the mesh in the straight pipes that are both annulus part and external part, the tube head part depended on its system and suitability. The independent parameters are shown in Figure 4.23.

The outer diameter of tube is 1.9 inch and inner diameter of tube is 1.774 inch. Diameters of sub-tube were changed in 2 cases to study temperature profiles.

Table 6 Dimensions of sub-tube of design 1 and 2

Design	ID (inch)	OD (inch)	Wall thickness (inch)
1	1.1149	1.315	0.083
2	0.824	1.05	0.113

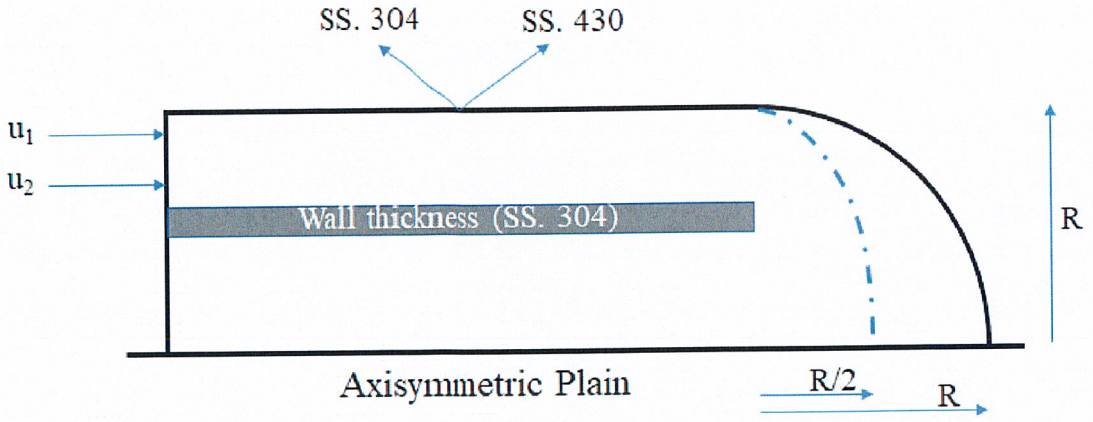

Figure 4.23 Independent parameters of heating media system calculations

Materials were set in the FLUNET step, the designs (tube sizes and tube head radius) were set in the GAMBIT. The final results could be checked in the report tool and displayed a faucet average of total temperature to measure the outlet temperature. They are shown as follows

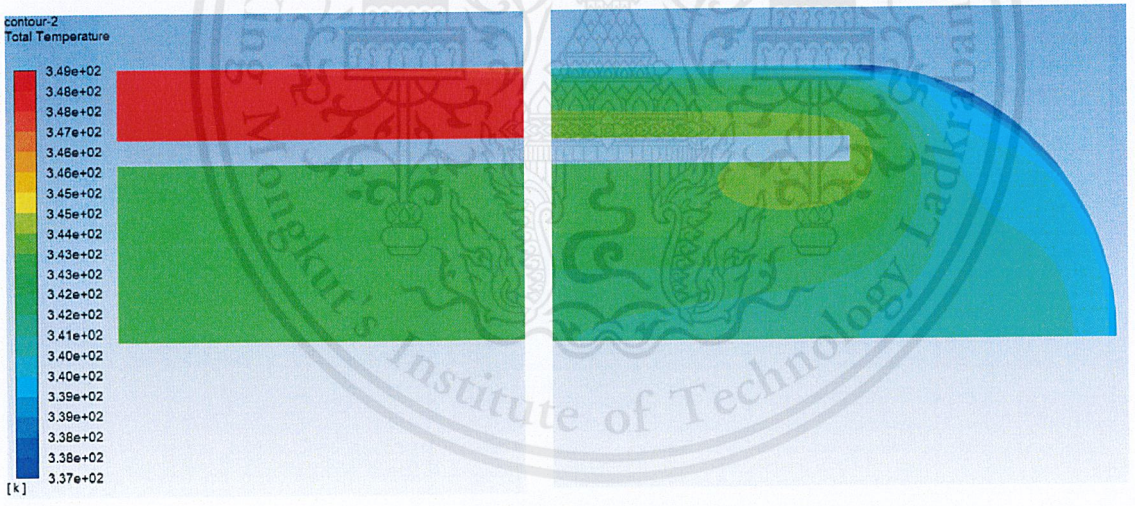

Figure 4.24 Temperature profiles of the design 1 containing stainless steel 304 of outer tube and tube head radius R design

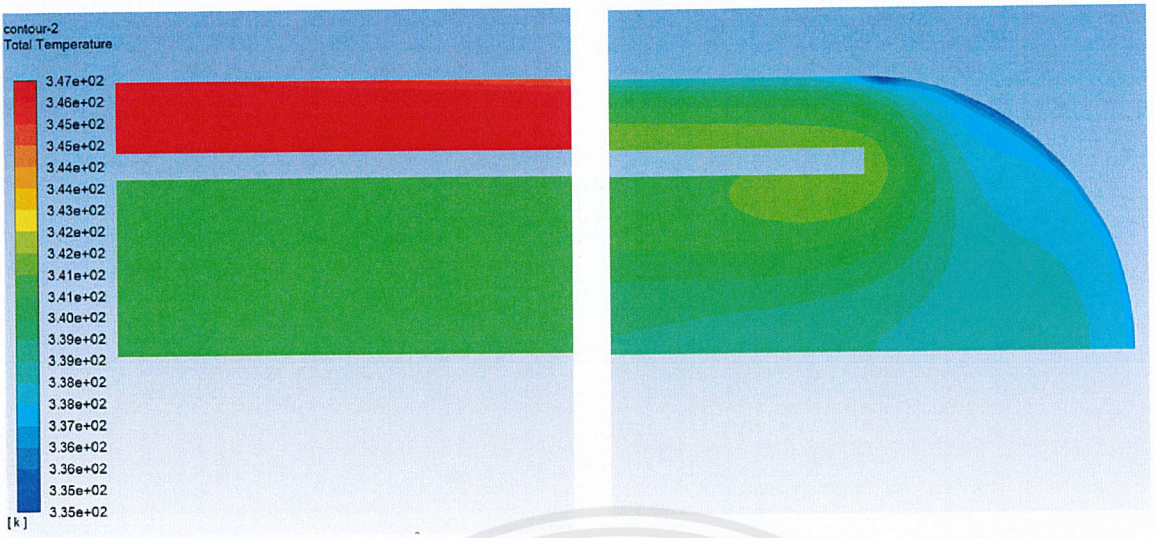

Figure 4.25 Temperature profiles of the design 1 containing stainless steel 403 of outer tube and tube head radius R design

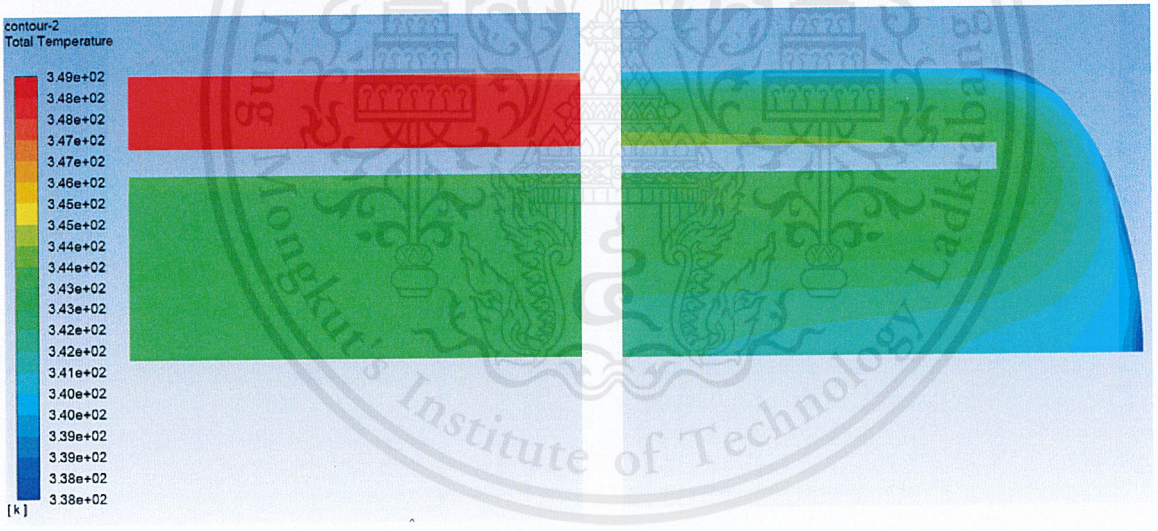

Figure 4.26 Temperature profiles of the design 1 containing stainless steel 304 of outer tube and tube head radius R/2 design

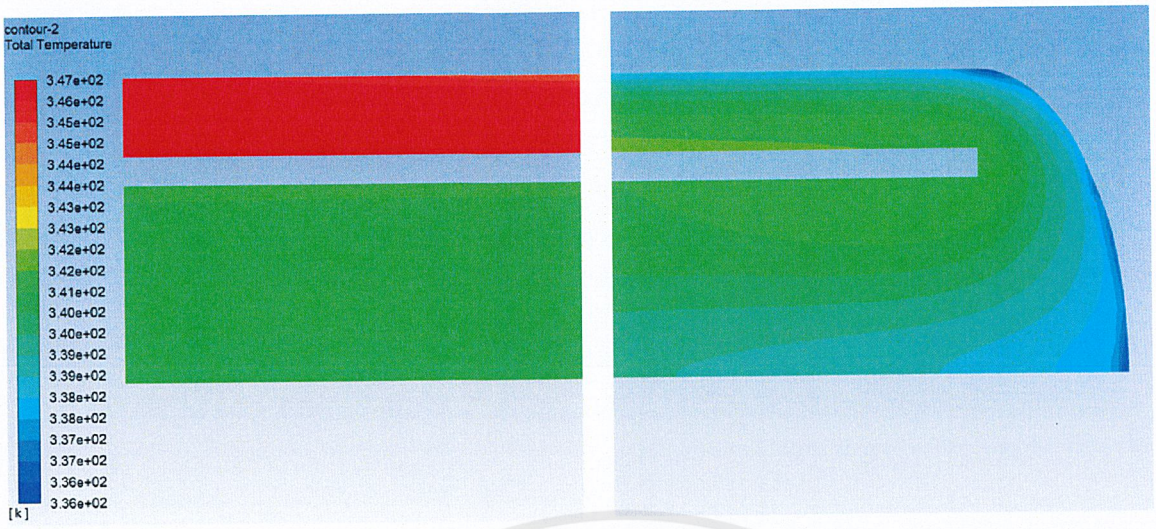

Figure 4.27 Temperature profiles of the design 1 containing stainless steel 403 of outer tube and tube head radius R/2 design

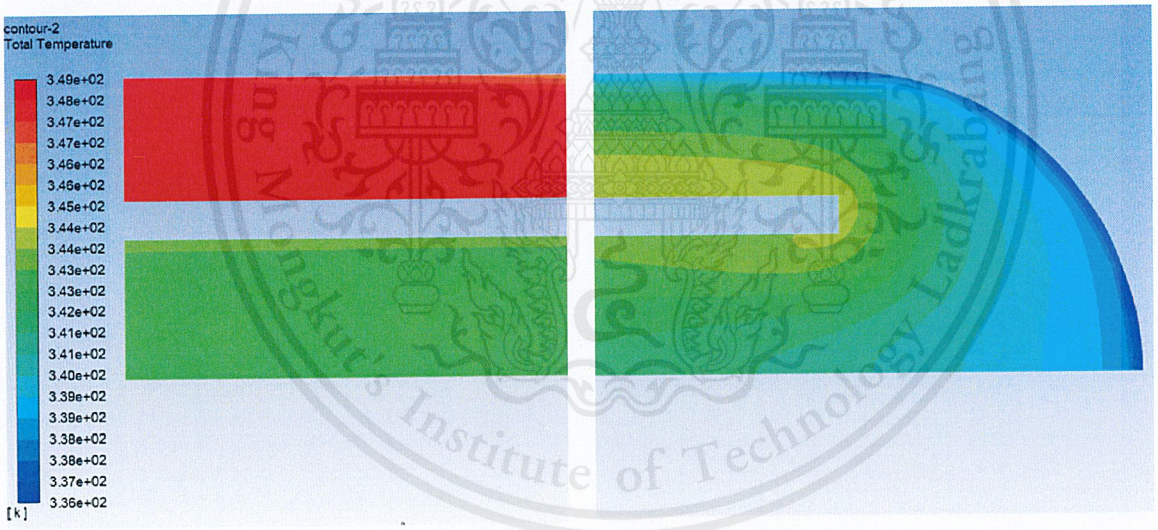

Figure 4.28 Temperature profiles of the design 2 containing stainless steel 304 of outer tube and tube head radius R design

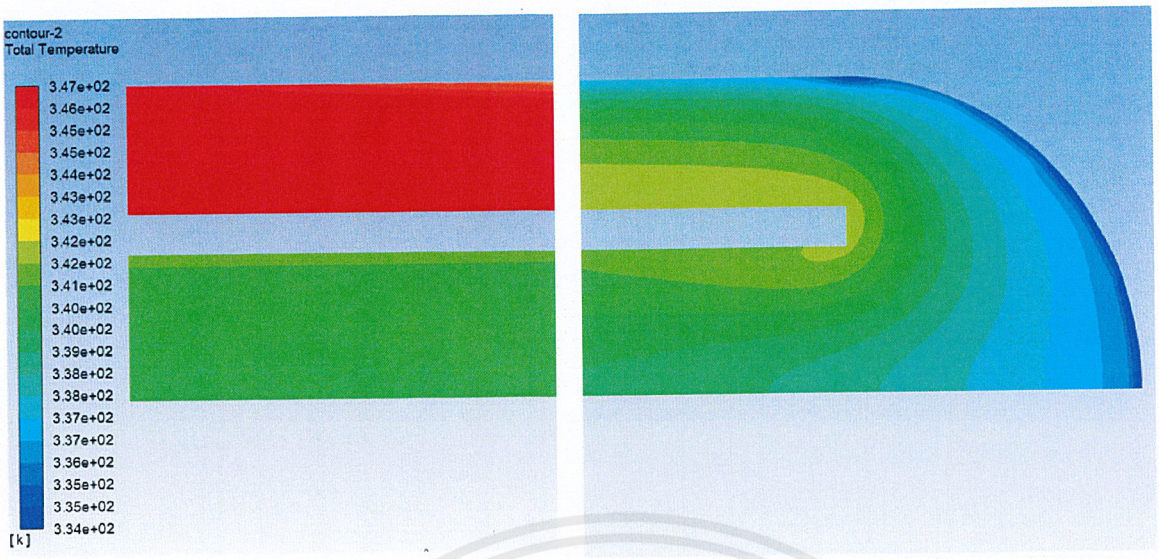

Figure 4.29 Temperature profiles of the design 2 containing stainless steel 403 of outer tube and tube head radius R design

Figure 4.30 Temperature profiles of the design 2 containing stainless steel 304 of outer tube and tube head radius R/2 design

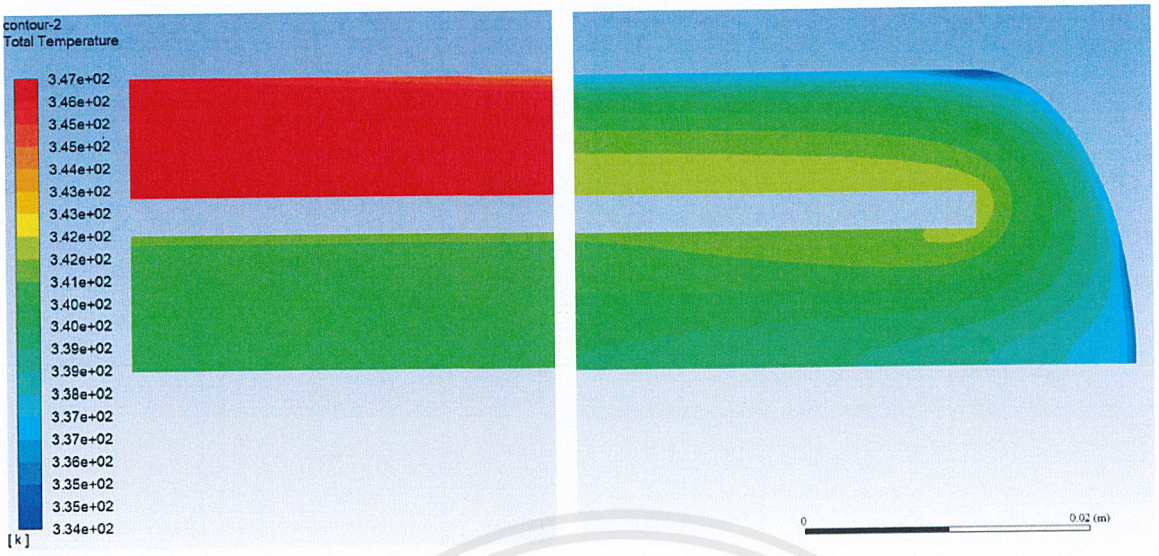

Figure 4.31 Temperature profiles of the design 2 containing stainless steel 403 of outer tube and tube head radius R/2 design

Table 7 Results from simulation by FLUENT

Design	Material	Tube Head Radius	Inlet Temperature (K)	Outlet Temperature (K)	Temperature Difference (K)	Improvement (%)
1	Stainless Steel 304	R	348.7369	342.9840	-5.7529	Reference
		R/2	348.7369	343.1052	-5.7217	-0.5423
	Stainless Steel 430	R	346.5019	340.5624	-5.9395	+3.2613
		R/2	346.5019	340.5987	-5.9032	+2.5305
2	Stainless Steel 304	R	348.7369	342.9954	-5.7415	-0.1931
		R/2	348.7369	343.0265	-5.7104	-0.7402
	Stainless Steel 430	R	346.5019	340.5753	-5.9266	+3.0418
		R/2	346.5019	340.6075	-5.8944	+2.2875

Temperature difference leads to proportional efficiency of heat transfer, high difference means the heat is conducted to the falling film plentifully. The results show that the temperature differences are little dissimilar, tendency of stainless steel 430 is better than another. Material of sub-tube is stainless steel 304, but the material of tube is varied. Stainless steel 430 not only requires less input temperature of hot water, but the rewarding input energy is also used. The main reason is thermal conductivity of stainless steel 430 (k = 27 W/m.K) is higher than stainless steel 304 (k = 16.27 W/m.K).

Velocity profiles can explain the heat transfer in turbulent flow, turbulent flows contain the high velocity and high variation, momentum transfer and heat transfer occur rapidly. That concludes heat transfer from the inlet part to the outlet part rises easily if it takes more turbulence. The outlet temperature in the case as design 1 is less than design 2. The design of R/2 tube head leads the better heat transfer for the inlet part, it is not necessary. It should unanimously choose the stainless steel to be the material of tube with design 1 and radius R of tube head. For examples, the velocity profile and turbulence of each case could be examined and compared by figure 4.32 and figure 4.33.

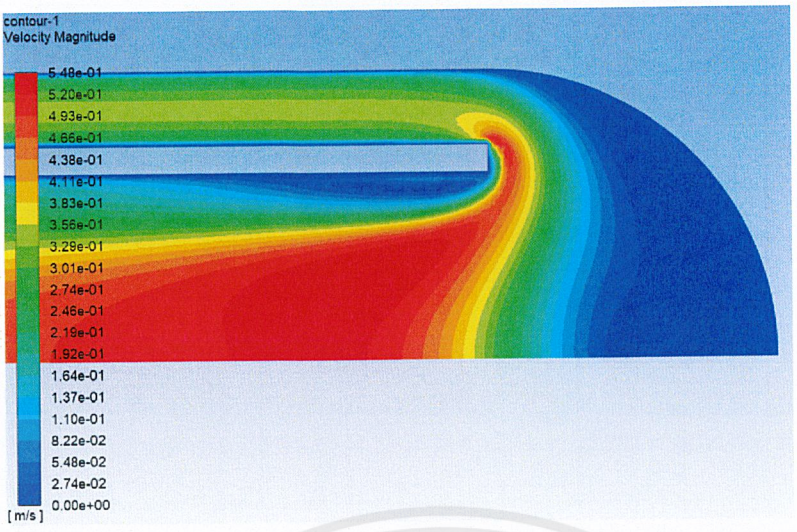

Figure 4.32 Velocity profiles of the design 1 containing stainless steel 403 of outer tube and tube head radius R design

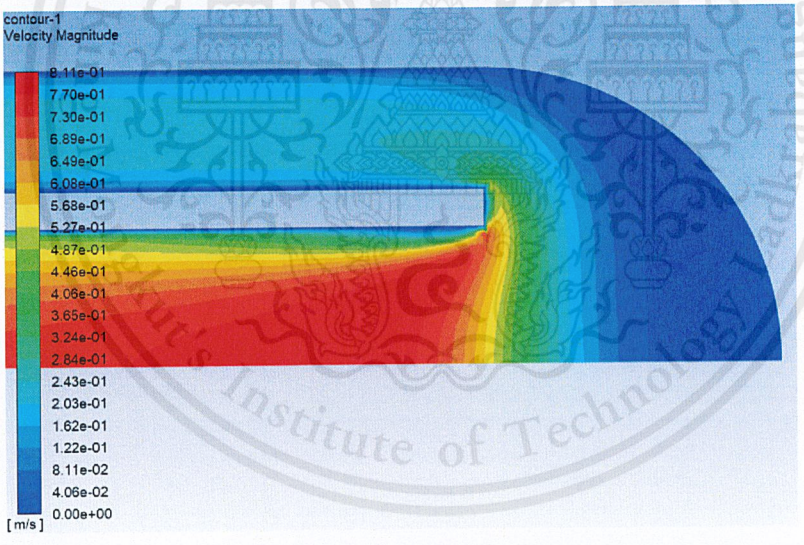

Figure 4.33 Velocity profiles of the design 2 containing stainless steel 403 of outer tube and tube head radius R design

4.4 System Improvement

The new 4-tube design is considered by the optimization involved the pressure drop and the rate of evaporation. However, the general evaporator design contains more hot tubes that is around 20 to 40 depended on the cross-sectional area of the evaporator. For this 8-inch shell design, it could be contained fully 10 tubes. The pressure drop of the general design is considered inside the tube while the pressure drop of the new design is calculated in the shell side. The comparison of the general design and new design shows in table 8.

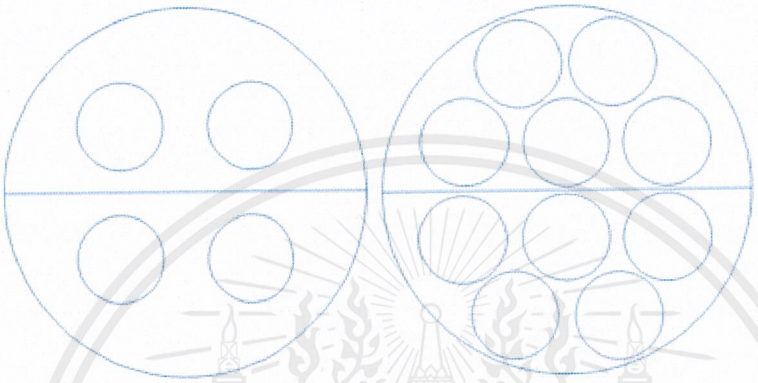

Figure 4.34 The actual ratio of shell and tube size for 4-tube and 10-tube design

Table 8 Comparison of the general design and new design

# of tubes	Design	Feed (kg/hr)	Rate (%) (No ΔP)	Pressure drop		Rate (%) (ΔP)
				Tube	Shell	
4	General design	94.3292	34.2925	78.9385	-	13.0031
	New design	101.0290	25.8644	-	3.9882	25.0876
10	General design	235.823	36.8660	78.9364	-	13.9871
	New design	252.5725	25.8632	-	30.1828	16.8889

The pressure drop of the general design is nearly constant while the number of hot tubes increases, but the new design take clearly increasing. The rate of evaporation is affected both designs by the pressure drop. When the effects of pressure drop involves, the new full developed design is still taken the advantage of rate of evaporation, which is above 3%.

Then, the effects of the number of tube variations for the new design are considered. The results show the advantage of the new design. If shell diameter is higher, the pressure drop would be lower. That is the proper design of the new design.

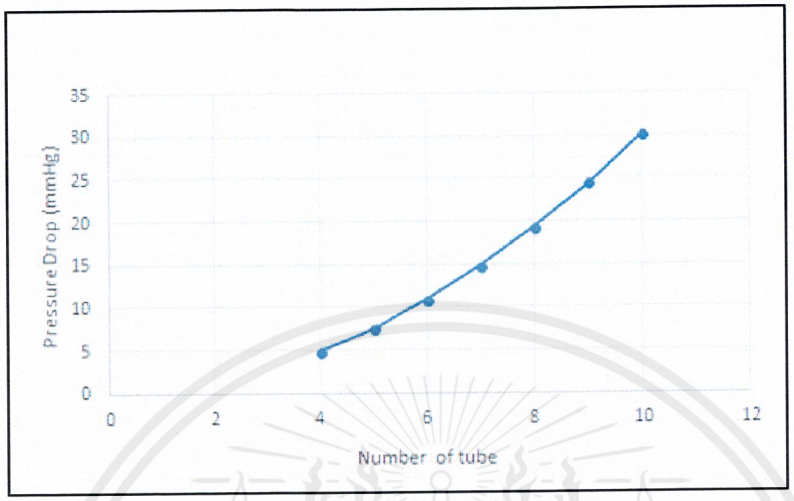

Figure 4.35 Effects of number of tube variations on pressure drop

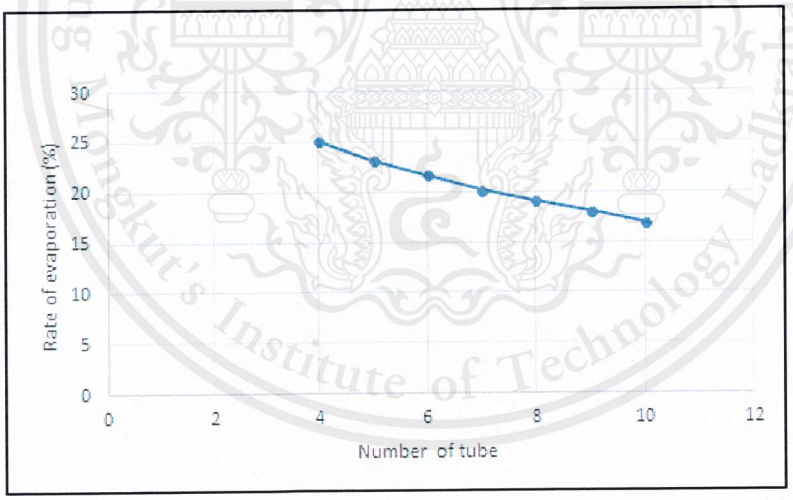

Figure 4.36 Effects of number of tube variations on rate of evaporation

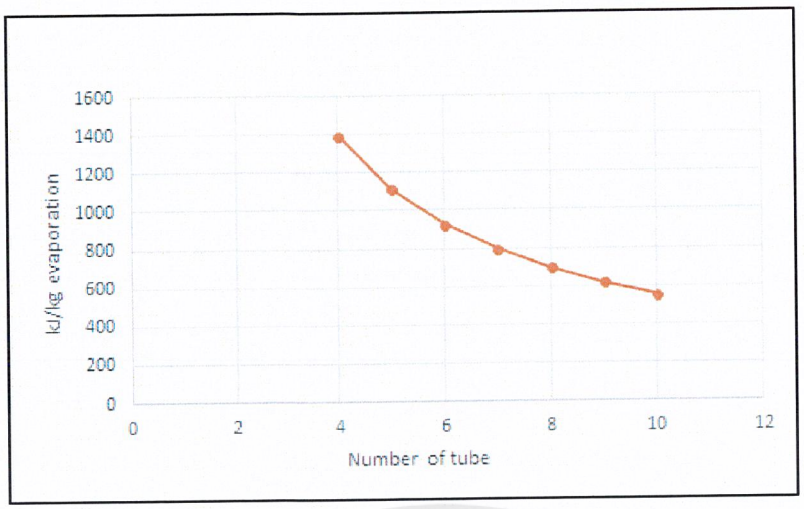

Figure 4.37 Effects of number of tube variations on ratio of energy requirement to mass of evaporation

The figure 4.37 show efficiency of the energy requirement. It would be properly optimized the number of hot tubes, if shell size is wider and the number of hot tube is more, curve would approach to be constant. When it is constant, the optimal required energy is the least case, and the system could be developed.

From the developed model, the falling film was improved by a collector. Collector addition could increase the outlet concentration or product concentration. The collector, well mixed producer, was longitudinal set at the middle of the heating tube, it could be increased the surface area of the falling film. It could develop the rate of evaporation of the falling film. The figure 4.38 shows the system without the collector, the film concentration profile is smooth. The heating tube with the collector could improve the rate of evaporation that shows in the figure 4.39.

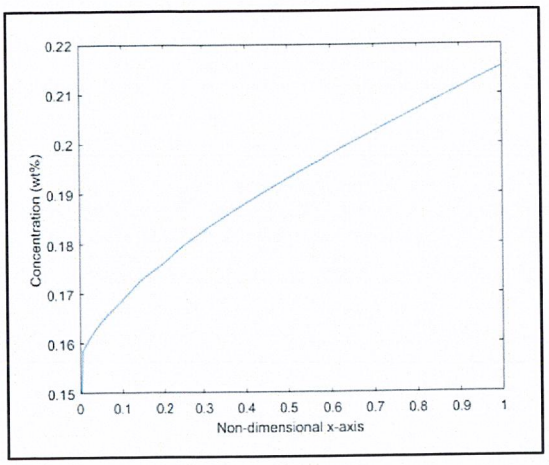

Figure 4.38 Concentration of the falling film without the collector for new design

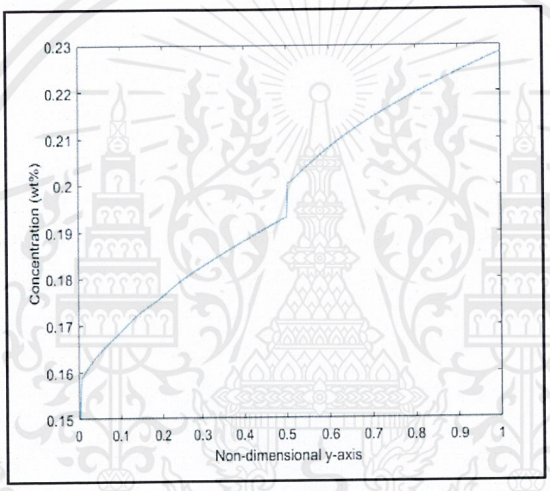

Figure 4.39 Concentration of the falling film with the collector for new design

The figure 4.39 shows that it changes in average concentration at the middle of the tube, the collector addition improves the concentration and evaporation immediately, and it is the previous tendency at the second-half part. The sugar solution layers are mixed to be a constant concentration solution at this point as ideal well mixed, and it can increase the concentration of the product.

CHAPTER V
CONCLUSION AND SUGESTION

The new design of falling film evaporator was created for pressure drop reduction. The 15 wt% of sugar solution was sampled with the heating media as hot water. Feed falling film was add at an outer tube surface continuously by a distributor and heating media system in the tube contained a small sub-tube which changed the hot water flow feed direction to the exit. 50.2 °C of sugur solution was fed counter flow with 73.4 °C of hot water. Concentration profiles of the falling film shown that the film was changed in concentration only 20-30% from its surface. Parameters involving shell and tube heat exchanger as number of tubes, tubes distribution, pressure drop and dimension of shell and tube were considered having an effect on rate of evaporator. The optimal shell dimensions were 8.625-inch of outer diameter and 8.071-inch of inner diameter, and the dimensions of tube were 1.9 inch of outer diameter and 1.774-inch of inner diameter. Efficiency of this system was led by the heat conduction of the wall thickness of the heating tube, so stainless steel 430 was better, its thermal conductivity is higher than stainless steel 304. This change could improve the efficiency of the energy input by over 3.2% from stainless steel 304 function. The materials of shell and sub-tube was still standard stainless steel 304, loss of heat transfer was less. Changing designs to design 2 caused the better flows motion, the outlet temperature was high and the energy used was not worthwhile. The overall of design 1 was used and packed by square pitch tubes been the furthermost of each and were not too closed to the shell surface in the same way. Operation was at 50 mmHg and took some pressure drop at 4.9882 mmHg. The system could produce 75.6832 kg/h of sugar solution from 101.0290 kg/h of feed falling film that is computed to 25.0876% rate of evaporation.

Main interesting parts of the falling film evaporator are the heating media system and the distributor part. This study has already considered, number of tubes and tubes distribution have designed by optimization for small system. The parameters still could be more varied to take the larger system and be more proper industrial scale. And for the distributor part, this study has not considered yet, the falling film still assumed that the study took continuous feed drops and required film characteristics.

References

[1] "Chapter 7 Evaporation," in *Industrial Technologies Program*, 2011, pp. 45–61.

[2] W. Li, X. Y. Wu, Z. Luo, and R. L. Webb, "Falling water film evaporation on newly-designed enhanced tube bundles," *Int. J. Heat Mass Transf.*, vol. 54, no. 13–14, pp. 2990–2997, 2011.

[3] S. Karami and B. Farhanieh, "A numerical study on the absorption of water vapor into a film of aqueous LiBr falling along a vertical plate," *Heat Mass Transf. und Stoffuebertragung*, vol. 46, no. 2, pp. 197–207, 2009.

[4] K. Lerssubsuree, "Modeling of an evaporator," King Mongkut's Institute of Technology Ladkrabang, 2016.

[5] GEA Wiegand GmbH, "Evaporation Technology," *Process Eng.*, p. 24, 2009.

[6] E. N. L. R. Byron Bird, Warren E. Stwwart, *Transport phenomena*. 2002.

[7] X. Bu, W. Ma, and Y. Huang, "Numerical study of heat and mass transfer of ammonia-water in falling film evaporator," *Heat Mass Transf.*, vol. 48, no. 5, pp. 725–734, 2012.

[8] J. M. Smith, H. C. Van Ness, M. M. Abbott, and M. T. Swihart, *Introduction to Chemical Engineering Thermodynamics*, Seventh. McGraw-Hill Education, 2017.

[9] S. Gaddis, "Pressure drop on the shell side of shell-and-tube with segmental baffles1 heat exchangers," *Chem. Eng. Process.*, vol. 36, 1997.

[10] D. Del Col, A. Muzzolon, P. Piubello, and L. Rossetto, "Measurement and prediction of evaporator shell-side pressure drop," *Int. J. Refrig.*, vol. 28, no. 3, pp. 320–330, 2005.

[11] R. E. Peters, M.S., Timmerhaus, K.D., and West, "Plant Design and Economics for Chemical Engineers, McGraw-Hill, New York," 2003.

[12] A. de La Calle, L. J. Yebra, and S. Dormido, "Modeling of a falling film evaporator," pp. 941–948, 2012.

[13] R. Krupiczka, A. Rotkegel, and Z. Ziobrowski, "Heat transfer to evaporating liquid films within a vertical tube," *Chem. Eng. Process.*, vol. 41, no. 1, pp. 23–28, 2002.

[14] C.-Y. Zhao, W.-T. Ji, P.-H. Jin, Y.-J. Zhong, and W.-Q. Tao, "Experimental study of the local and average falling film evaporation coefficients in a horizontal enhanced tube bundle using R134a," *Appl. Therm. Eng.*, vol. 129, no. Supplement C, pp. 502–511, 2018.

[15] F. Liu, D. Wang, Q. Wang, and J. Ga, "The optimum design of falling-film evaporator and numerical simulation of distributor," *Procedia Eng.*, vol. 205, pp. 3867–3872, 2017.

APPENDIX

APPENDIX A

Properties of Fluids and Materials

15 wt% of Sugar solution at 50 °C

Density	: 1,056 kg/m^3
Viscosity	: 1.23 x 10^{-3} kg/m.s
Specific Heat Capacity	: 2,432.159 kJ/kg.K
Thermal Conductivity	: 0.353 W/m.K
Diffusivity Coefficient	: 5.02 x 10^{-10} m^2/s

Liquid water at 70 °C

Density	: 975.8 kg/m^3
Viscosity	: 3.87 x 10^{-3} kg/m.s

Stainless steel 304

Thermal Conductivity	: 16.27 W/m.K

Stainless steel 430

Thermal Conductivity	: 27 W/m.K

APPENDIX B

Raw Data of Pressure Drop Calculations

Table 9 Pressure drop for k = 0.90 at 40 mmHg

Shell (inch)	Square pitch		Triangular pitch	
	Tube OD (inch)	Pressure drop (mmHg)	Tube OD (inch)	Pressure drop (mmHg)
8	3/4	0.166	3/4	0.0114
	1	0.5736	1	0.2104
	5/4	1.5205	5/4	0.5475
	3/2	3.442	3/2	1.2157
	2	13.6386	2	4.6178
10	3/4	0.0648	3/4	0.0245
	1	0.2237	1	0.0833
	5/4	0.5873	5/4	0.2154
	3/2	1.3033	3/2	0.4711
	2	4.767	2	1.6704
12	3/4	0.03	3/4	0.0114
	1	0.1038	1	0.039
	5/4	0.2721	5/4	0.101
	3/2	0.6	3/2	0.2201
	2	2.1302	2	0.7623
15	3/4	0.0116	3/4	0.0044
	1	0.0405	1	0.0154
	5/4	0.1096	5/4	0.04
	3/2	0.2341	3/2	0.0871
	2	0.8186	2	0.2989

Table 10 Pressure drop for k = 0.95 at 40 mmHg

Shell (inch)	Square pitch		Triangular pitch	
	Tube OD (inch)	Pressure drop (mmHg)	Tube OD (inch)	Pressure drop (mmHg)
8	3/4	0.1444	3/4	0.0536
	1	0.4978	1	0.1815
	5/4	1.3133	5/4	0.4704
	3/2	2.9484	3/2	1.0364
	2	11.3111	2	3.8183
10	3/4	0.0564	3/4	0.0211
	1	0.1945	1	0.072
	5/4	0.5097	5/4	0.1859
	3/2	1.127	3/2	0.4052
	2	4.065	2	1.418
12	3/4	0.026	3/4	0.0098
	1	0.0903	1	0.0337
	5/4	0.2366	5/4	0.0873
	3/2	0.5207	3/2	0.1899
	2	1.8355	2	0.6535
15	3/4	0.0101	3/4	0.0038
	1	0.0352	1	0.0133
	5/4	0.0925	5/4	0.0345
	3/2	0.2036	3/2	0.0753
	2	0.7097	2	0.2577

Table 11 Pressure drop for k = 1.00 at 40 mmHg

Shell (inch)	Square pitch		Triangular pitch	
	Tube OD (inch)	Pressure drop (mmHg)	Tube OD (inch)	Pressure drop (mmHg)
8	3/4	0.1264	3/4	0.0466
	1	0.4350	1	0.1577
	5/4	1.1435	5/4	0.4073
	3/2	2.5509	3/2	0.8921
	2	9.5555	2	3.2135
10	3/4	0.0493	3/4	0.0184
	1	0.1702	1	0.0626
	5/4	0.4455	5/4	0.1615
	3/2	0.9822	3/2	0.3512
	2	3.5050	2	1.2167
12	3/4	0.0228	3/4	0.0086
	1	0.0790	1	0.0293
	5/4	0.2070	5/4	0.0759
	3/2	0.4551	3/2	0.1650
	2	1.5953	2	0.5649
15	3/4	0.0088	3/4	0.0033
	1	0.0308	1	0.0115
	5/4	0.0809	5/4	0.0301
	3/2	0.1781	3/2	0.0655
	2	0.6198	2	0.2237

Table 12 Pressure drop for k = 1.05 at 40 mmHg

Shell (inch)	Square pitch		Triangular pitch	
	Tube OD (inch)	Pressure drop (mmHg)	Tube OD (inch)	Pressure drop (mmHg)
8	3/4	0.1368	3/4	0.0506
	1	0.4713	1	0.1715
	5/4	1.2414	5/4	0.4436
	3/2	2.7794	3/2	0.975
	2	10.5529	2	3.5572
10	3/4	0.0534	3/4	0.02
	1	0.1843	1	0.068
	5/4	0.4826	5/4	0.1756
	3/2	1.0658	3/2	0.3823
	2	3.8264	2	1.3322
12	3/4	0.0247	3/4	0.0093
	1	0.0855	1	0.0319
	5/4	0.2241	5/4	0.0825
	3/2	0.493	3/2	0.1794
	2	1.7337	2	0.6159
15	3/4	0.0095	3/4	0.0036
	1	0.0333	1	0.0125
	5/4	0.0876	5/4	0.0326
	3/2	0.1928	3/2	0.0712
	2	0.6717	2	0.2433

Table 13 Pressure drop for k = 1.10 at 40 mmHg

Shell (inch)	Square pitch		Triangular pitch	
	Tube OD (inch)	Pressure drop (mmHg)	Tube OD (inch)	Pressure drop (mmHg)
8	3/4	0.1569	3/4	0.0584
	1	0.5415	1	0.1981
	5/4	1.4324	5/4	0.5147
	3/2	3.231	3/2	1.1391
	2	12.6224	2	4.2691
10	3/4	0.0612	3/4	0.0231
	1	0.2114	1	0.0785
	5/4	0.5545	5/4	0.2029
	3/2	1.2285	3/2	0.4431
	2	4.466	2	1.5622
12	3/4	0.0283	3/4	0.0107
	1	0.0981	1	0.0368
	5/4	0.2571	5/4	0.0952
	3/2	0.5664	3/2	0.2073
	2	2.0047	2	0.7159
15	3/4	0.011	3/4	0.0042
	1	0.0382	1	0.0145
	5/4	0.1005	5/4	0.0377
	3/2	0.2212	3/2	0.0821
	2	0.7724	2	0.2814

Table 14 Pressure drop for k = 1.00 at 50 mmHg

Shell (inch)	Square pitch		Triangular pitch	
	Tube OD (inch)	Pressure drop (mmHg)	Tube OD (inch)	Pressure drop (mmHg)
8	3/4	0.133	3/4	0.0491
	1	0.4561	1	0.1654
	5/4	1.1945	5/4	0.4255
	3/2	2.6566	3/2	0.9291
	2	9.8984	2	3.3288
10	3/4	0.0519	3/4	0.0193
	1	0.1785	1	0.0656
	5/4	0.4653	5/4	0.1687
	3/2	1.0229	3/2	0.3657
	2	3.6308	2	1.2603
12	3/4	0.024	3/4	0.009
	1	0.0828	1	0.0307
	5/4	0.2162	5/4	0.0793
	3/2	0.4739	3/2	0.1719
	2	1.6525	2	0.5852
15	3/4	0.0093	3/4	0.0035
	1	0.0323	1	0.0121
	5/4	0.0846	5/4	0.0314
	3/2	0.1855	3/2	0.0682
	2	0.642	2	0.2317

Table 15 Pressure drop for k = 1.00 at 60 mmHg

Shell (inch)	Square pitch		Triangular pitch	
	Tube OD (inch)	Pressure drop (mmHg)	Tube OD (inch)	Pressure drop (mmHg)
8	3/4	0.1386	3/4	0.0511
	1	0.4739	1	0.1718
	5/4	1.2378	5/4	0.4409
	3/2	2.7464	3/2	0.9605
	2	10.1908	2	3.4271
10	3/4	0.0541	3/4	0.0202
	1	0.1854	1	0.0682
	5/4	0.4822	5/4	0.1748
	3/2	1.0575	3/2	0.3781
	2	3.7380	2	1.2976
12	3/4	0.0250	3/4	0.0094
	1	0.0861	1	0.0319
	5/4	0.2240	5/4	0.0822
	3/2	0.4899	3/2	0.1777
	2	1.7013	2	0.6024
15	3/4	0.0097	3/4	0.0037
	1	0.0335	1	0.0126
	5/4	0.0876	5/4	0.0325
	3/2	0.1918	3/2	0.0705
	2	0.6609	2	0.2386

Table 16 Rate of evaporation at 40 mmHg

Shell (inch)	Square pitch		Triangular pitch	
	Tube OD (inch)	Rate of evaporation (%)	Tube OD (inch)	Rate of evaporation (%)
8	3/4	35.7379	3/4	35.8206
	1	33.6215	1	33.6711
	5/4	31.2789	5/4	31.4143
	3/2	28.9183	3/2	29.6691
	2	23.6081	2	25.9078
10	3/4	35.9821	3/4	35.9880
	1	33.7433	1	33.7613
	5/4	31.5877	5/4	31.6237
	3/2	29.5232	3/2	29.7894
	2	25.4700	2	26.2237
12	3/4	36.0967	3/4	36.1072
	1	33.7833	1	33.8516
	5/4	31.6743	5/4	31.7032
	3/2	29.7263	3/2	29.8496
	2	26.1064	2	26.4494
15	3/4	36.1057	3/4	36.1084
	1	33.8126	1	33.8516
	5/4	31.7388	5/4	31.7754
	3/2	29.8391	3/2	29.8797
	2	26.4415	2	26.5848

Table 17 Rate of evaporation at 50 mmHg

Shell (inch)	Square pitch		Triangular pitch	
	Tube OD (inch)	Rate of evaporation (%)	Tube OD (inch)	Rate of evaporation (%)
8	3/4	31.5492	3/4	31.5907
	1	29.4859	1	29.6011
	5/4	27.4756	5/4	27.7508
	3/2	25.4464	3/2	25.9889
	2	20.8555	2	22.5367
10	3/4	31.5893	3/4	31.5922
	1	29.6210	1	29.6367
	5/4	27.7318	5/4	27.8353
	3/2	25.9577	3/2	26.1652
	2	22.4664	2	23.1151
12	3/4	31.5898	3/4	31.5973
	1	29.6282	1	29.6406
	5/4	27.8125	5/4	27.8655
	3/2	26.1395	3/2	26.2317
	2	22.9989	2	23.3005
15	3/4	31.5971	3/4	31.6000
	1	29.6398	1	29.6497
	5/4	27.8629	5/4	27.8886
	3/2	26.2271	3/2	26.2683
	2	23.2868	2	23.4022

Table 18 Rate of evaporation at 60 mmHg

Shell (inch)	Square pitch		Triangular pitch	
	Tube OD (inch)	Rate of evaporation (%)	Tube OD (inch)	Rate of evaporation (%)
8	3/4	27.8638	3/4	27.8870
	1	26.0740	1	26.1636
	5/4	24.3270	5/4	24.5561
	3/2	22.5408	3/2	23.0347
	2	18.5184	2	20.0191
10	3/4	27.8857	3/4	27.8997
	1	26.1662	1	26.2012
	5/4	24.5522	5/4	24.6378
	3/2	23.0091	3/2	23.1901
	2	19.9401	2	20.5196
12	3/4	27.8977	3/4	27.9042
	1	26.1939	1	26.2160
	5/4	24.6306	5/4	24.6624
	3/2	23.1582	3/2	23.2449
	2	20.4136	2	20.6782
15	3/4	27.9041	3/4	27.9065
	1	26.2150	1	26.2239
	5/4	24.6602	5/4	24.6825
	3/2	23.2392	3/2	23.2751
	2	20.6671	2	20.7711

Table 19 Feed and product at 40 mmHg for square pitch type

Shell (inch)	Square pitch				
	Tube OD (inch)	Feed (kg/hr)	Product (kg/hr)	Product concentration (wt%)	Evaporation/heat duty (g/kJ)
8	3/4	39.8798	25.6277	23.3419	0.1934
	1	53.1731	35.2956	22.5977	0.1901
	5/4	66.4664	45.6765	21.8274	0.1868
	3/2	79.7597	56.6945	21.1025	0.1837
	2	106.346	81.2399	19.6356	0.1764
10	3/4	39.8798	25.5303	23.4309	0.1935
	1	53.1731	35.2308	22.6392	0.1900
	5/4	66.4664	45.4713	21.9259	0.1868
	3/2	79.7597	56.2121	21.2836	0.1837
	2	106.3463	79.2599	20.1261	0.1773
12	3/4	39.8798	25.4846	23.4730	0.1935
	1	53.1731	35.2095	22.6529	0.1900
	5/4	66.4664	45.4137	21.9537	0.1869
	3/2	79.7597	56.0501	21.3451	0.1836
	2	106.346	78.5831	20.2995	0.1772
15	3/4	39.8798	25.4810	23.4763	0.1935
	1	53.1731	35.1939	22.6629	0.1902
	5/4	66.4664	45.3708	21.9744	0.1869
	3/2	79.7597	55.9601	21.3794	0.1836
	2	106.3463	78.2267	20.3919	0.1772

Table 20 Feed and product at 40 mmHg for triangular pitch type

Shell (inch)	Triangular pitch				
	Tube OD (inch)	Feed (kg/hr)	Product (kg/hr)	Product concentration (wt%)	Evaporation/heat duty (g/kJ)
8	3/4	29.9099	19.1960	23.3720	0.1936
	1	39.8799	26.4519	22.6146	0.1894
	5/4	49.8498	34.1898	21.8705	0.1864
	3/2	59.8198	42.0718	21.3278	0.1831
	2	79.7597	59.0957	20.2450	0.1778
10	3/4	29.9099	19.1459	23.4331	0.1938
	1	39.8799	26.4159	22.6454	0.1899
	5/4	49.8498	34.0854	21.9374	0.1866
	3/2	59.8198	41.9998	21.3643	0.1836
	2	79.7597	58.8437	20.3317	0.1778
12	3/4	29.9099	19.1103	23.4768	0.1942
	1	39.8799	26.3799	22.6763	0.1899
	5/4	49.8498	34.0458	21.9630	0.1867
	3/2	59.8198	41.9638	21.3826	0.1837
	2	79.7597	58.6637	20.3941	0.1778
15	3/4	29.9099	19.1099	23.4773	0.1942
	1	39.8799	26.3799	22.6763	0.1902
	5/4	49.8498	34.0098	21.9862	0.1869
	3/2	59.8198	41.9458	21.3918	0.1835
	2	79.7597	58.5557	20.4317	0.1778

Table 21 Feed and product at 50 mmHg for square pitch type

Shell (inch)	Square pitch				
	Tube OD (inch)	Feed (kg/hr)	Product (kg/hr)	Product concentration (wt%)	Evaporation/heat duty (g/kJ)
8	3/4	39.8798	27.2981	21.9136	0.1932
	1	53.1731	37.4946	21.2724	0.1901
	5/4	66.4664	48.2044	20.6827	0.1867
	3/2	79.7597	59.4637	20.1198	0.1837
	2	106.346	84.1672	18.9527	0.1762
10	3/4	39.8798	27.2821	21.9264	0.1931
	1	53.1731	37.4227	21.3132	0.1901
	5/4	66.4664	48.0341	20.7560	0.1869
	3/2	79.7597	59.0559	20.2587	0.1836
	2	106.3463	82.4540	19.3465	0.1769
12	3/4	39.8798	27.2819	21.9266	0.1931
	1	53.1731	37.4189	21.3154	0.1902
	5/4	66.4664	47.9805	20.7792	0.1870
	3/2	79.7597	58.9109	20.3086	0.1837
	2	106.346	81.8878	19.4803	0.1773
15	3/4	39.8798	27.2790	21.9289	0.1932
	1	53.1731	37.4127	21.3189	0.1900
	5/4	66.4664	47.9469	20.7938	0.1868
	3/2	79.7597	58.8410	20.3327	0.1836
	2	106.3463	81.5816	19.5534	0.1772

Table 22 Feed and product at 50 mmHg for triangular pitch type

Shell (inch)	Triangular pitch				
	Tube OD (inch)	Feed (kg/hr)	Product (kg/hr)	Product concentration (wt%)	Evaporation/heat duty (g/kJ)
8	3/4	29.9099	20.4611	21.9269	0.1931
	1	39.8799	28.0750	21.3072	0.1903
	5/4	49.8498	36.0161	20.7615	0.1870
	3/2	59.8198	44.2733	20.2672	0.1837
	2	79.7597	61.7845	19.3640	0.1771
10	3/4	29.9099	20.4607	21.9273	0.1931
	1	39.8799	28.0608	21.3179	0.1902
	5/4	49.8498	35.9739	20.7858	0.1869
	3/2	59.8198	44.1678	20.3156	0.1835
	2	79.7597	61.3231	19.5097	0.1773
12	3/4	29.9099	20.4592	21.9290	0.1932
	1	39.8799	28.0592	21.3191	0.1900
	5/4	49.8498	35.9589	20.7945	0.1869
	3/2	59.8198	44.1280	20.3339	0.1836
	2	79.7597	61.1753	19.5569	0.1771
15	3/4	29.9099	20.4584	21.9298	0.1932
	1	39.8799	28.0556	21.3219	0.1900
	5/4	49.8498	35.9474	20.8012	0.1870
	3/2	59.8198	44.1061	20.3441	0.1837
	2	79.7597	61.0942	19.5828	0.1772

Table 23 Feed and product at 60 mmHg for square pitch type

Shell (inch)	Square pitch				
	Tube OD (inch)	Feed (kg/hr)	Product (kg/hr)	Product concentration (wt%)	Evaporation/heat duty (g/kJ)
8	3/4	39.8798	28.7678	20.7940	0.1928
	1	53.1731	39.3084	20.2908	0.1900
	5/4	66.4664	50.2971	19.8221	0.1868
	3/2	79.7597	61.7812	19.3650	0.1836
	2	106.346	86.6526	18.4091	0.1766
10	3/4	39.8798	28.7591	20.8003	0.1929
	1	53.1731	39.2597	20.3159	0.1901
	5/4	66.4664	50.1474	19.8813	0.1869
	3/2	79.7597	61.4077	19.4828	0.1838
	2	106.3463	85.1408	18.7360	0.1773
12	3/4	39.8798	28.7543	20.8038	0.1930
	1	53.1731	39.2450	20.3235	0.1900
	5/4	66.4664	50.0953	19.9020	0.1870
	3/2	79.7597	61.2888	19.5206	0.1839
	2	106.346	84.6372	18.8474	0.1772
15	3/4	39.8798	28.7518	20.8056	0.1931
	1	53.1731	39.2336	20.3294	0.1901
	5/4	66.4664	50.0756	19.9098	0.1870
	3/2	79.7597	61.2242	19.5412	0.1839
	2	106.3463	84.3669	18.9078	0.1773

Table 24 Feed and product at 60 mmHg for triangular pitch type

Shell (inch)	Triangular pitch				
	Tube OD (inch)	Feed (kg/hr)	Product (kg/hr)	Product concentration (wt %)	Evaporation/heat duty (g/kJ)
8	3/4	29.9099	21.5689	20.8007	0.1929
	1	39.8799	29.4458	20.3152	0.1901
	5/4	49.8498	37.6086	19.8823	0.1867
	3/2	59.8198	46.0404	19.4893	0.1838
	2	79.7597	63.7926	18.7545	0.1774
10	3/4	29.9099	21.5651	20.8044	0.1930
	1	39.8799	29.4309	20.3255	0.1900
	5/4	49.8498	37.5679	19.9039	0.1868
	3/2	59.8198	45.9475	19.5287	0.1837
	2	79.7597	63.3933	18.8726	0.1774
12	3/4	29.9099	21.5638	20.8057	0.1931
	1	39.8799	29.4249	20.3296	0.1901
	5/4	49.8498	37.5556	19.9104	0.1867
	3/2	59.8198	45.9147	19.5427	0.1837
	2	79.7597	63.2668	18.9103	0.1774
15	3/4	29.9099	21.5631	20.8063	0.1931
	1	39.8799	29.4218	20.3318	0.1902
	5/4	49.8498	37.5456	19.9157	0.1869
	3/2	59.8198	45.8966	19.5504	0.1837
	2	79.7597	63.1927	18.9325	0.1773

APPENDIX C

MATLAB Codes

MATLAB codes

```
% Initial assume for iteration
        mevap2 = 1.0E-5;                % First assume

% Grid [roll(M) collumn(N)]

%     M = 200; N = 10;                  % Vary size of grid
   M = 300; N = 20;
%     M = 400; N = 30;

   dy = 1/N; dx = 1/M;
   n = 1:M; i = 1:N;
   MN = [M N];

% Properties of 15wt% sugar solution @323.15 K or @50 oC
   Tin = 50+273.15;          % [K] initial sugar solution temperature
   win = 0.15;
   rho = 1056;               % [kg/m^3] density %
   Cp = 2722;                % [J/(kg.K)] specific heat %
   ks = 0.353;               % [W/(m.K)] thermal conductivity of solution
   Dm = 5.02E-10;            % [m^2/s] diffusivity of solution
   vis = 1.234E-3;           % [kg/(m.s)] viscosity of solution
   divis = vis/rho;          % [m^2/s] dinamic viscosity of solution
   Hfg = 2432158.945;        % [J/kg] latent heat of solution
   alpha = ks/(rho*Cp);      % [m^2/s]

 % Dimension of a tube and properties
   L = 1;                  % [m] length of tube

% General constants
   g = 9.81;                                  % [g/m^2] gravity acceleration
   Re = 150;                                  % [-] initial reynolds number
   tal0 = Re*vis/4;                           % [m]
   thick0 = (3*tal0*divis/(g*rho)).^(1/3);    % [m]

   mhot = 0.2;
   Cphot = 4187;
   mCphot = mhot*Cphot;
   rhoheat = 975.8;

 %  Variables
   tal = zeros(M+1,1);
   talevapA = zeros(M,1);
   mevap = mevap2.*ones(M,1);
   mevapA = zeros(M,1);
   tal(1) = tal0;
   thick = zeros(M,1);
   thick(1) = thick0;
   T = zeros(M,N);
```

```
w = zeros(M,N);
ne(i) = i*dy;
ab(n) = n*dx;
zhot = 1;
z = 1;
zz = 1;
tolerancez = ones(M,1);
tolerancezz = ones(M,1);
tolerancezhot = ones(M,1);
Twall = zeros(M,1);
w(1,i) = win;
w(n,1) = win;
T(n,1) = Twall;
T(1,i) = Tin;

% Antoine Equation
A = zeros(M,1);
B = zeros(M,1);
C = zeros(M,1);

P = 50;
Thot0 = 60 + 273.15;          % Assume
Thot = Thot0.*ones(M,1);      % Define outlet temp
Thotout = Thot(2);
wavg = zeros(M,1);
wavg(1) = win;

%++++++++++++++++++++++++++++++++++++++++++++++++++++++++++++++++++++++++++++

    Ds = 0.0254*8.071;        %Vary+++++
    D = 0.0254*1.9;           %Vary+++++


    PSq = (Ds + D)/(2 + sqrt(2));
    cSq = PSq - D;
    SqSq = PSq;
    SLSq = PSq;

    %Standard [TubeOD Pitch Clearance]
    Sq1 = [3/4*0.0254 PSq cSq];
    Sq2 = [1*0.0254 PSq cSq];
    Sq3 = [(1+1/4)*0.0254 PSq cSq];
    Sq4 = [(1+1/2)*0.0254 PSq cSq];
    Sq5 = [2*0.0254 PSq cSq];
    CSq = 1;

    aSq = SqSq/D;
    bSq = SLSq/D;
    cSq = sqrt((aSq/2)^2+(bSq)^2);
```

```
rSq = PSq/sqrt(2);

a = aSq;
b = bSq;
c = cSq;

%++++++++++++++++++++++++++++++++++++++++++++++++++++++++++++++++++++++++++++++

Y = 0.00001;
Thotin = 70 + 273.15;
error = 0.00010001;
while error > 0.0001

for n = 2:M*0.5

   while tolerancez(n) > 0.0001
      T(n,1) = Thot(n);

         while tolerancezz(n) > 0.0001
            mevapA(n) = mevap(n);
            talevapA(n) = mevapA(n)*dx;
            tal(n) = tal(n-1) - talevapA(n);
            dtal(n) = tal(n) - tal(n-1);
            thick(n) = (3*tal(n)*divis/(g*rho)).^(1/3);
            dthick(n) = thick(n) - thick(n-1);

               for i = 2:N-1
                  u(n,i) = ((rho.*g.*thick(n).^2)./(2*vis)).*(2.*ne(i) - ne(i).^2);
                  v(n,i) = -
1.*((rho*g^2)./(74.*vis^2.*tal(n).^2)).^(1/3).*((thick(n).^2).*(ne(i).^2).*dtal(n))./(L*dx);
               end

               for i = 2:N-1
                  aheat(n,i) = ((ne(i).*dthick(n)./(thick(n).*dx)) -
(v(n,i).*L./(u(n,i).*thick(n)))).*dx/dy;
                  bheat(n,i) = (alpha*L./(u(n,i).*thick(n).^2)).*(dx/(dy^2));
                  amass(n,i) = ((ne(i).*dthick(n)./(thick(n).*dx)) -
(v(n,i).*L./(u(n,i).*thick(n)))).*dx/dy;
                  cmass(n,i) = (Dm*L./(u(n,i).*thick(n).^2)).*(dx/(dy^2));

                  Aheat(n,i) = bheat(n,i);
                  Bheat(n,i) = (1 - aheat(n,i) - 2.*bheat(n,i));
                  Cheat(n,i) = aheat(n,i) + bheat(n,i);

                  Amass(n,i) = cmass(n,i);
                  Bmass(n,i) = (1 - amass(n,i) - 2.*cmass(n,i));
                  Cmass(n,i) = amass(n,i) + cmass(n,i);
               end
```

```
            for i = 2:N-1
              T(n,i) = Aheat(n,i).*T(n-1,i-1) + Bheat(n,i).*T(n-1,i)
                    + Cheat(n,i).*T(n-1,i+1);
               w(n,i) = Amass(n,i).*w(n-1,i-1) + Bmass(n,i).*w(n-1,i)
                    + Cmass(n,i).*w(n-1,i+1);
            end

          J = mevapA(n).*thick(n).*dy./(rho*Dm) ;
          w(n,N) = (J + w(n,N-1))./(J + 1) ;

          A(n) = 7.944 - 0.4728.*w(n,N) + 1.847.*w(n,N).^2 - 2.526.*w(n,N).^3 ;
          B(n) = 1653 - 264.9.*w(n,N) + 1158.*w(n,N).^2 - 1497.*w(n,N).^3 ;
          C(n) = 226.7 - 29.01.*w(n,N) + 126.2.*w(n,N).^2 - 164.2.*w(n,N).^3 ;
          T(n,N) = -(B(n)./(log10(P)-A(n))) - C(n) + 273.15 ;
          mevap(n) = -ks.*(T(n,N) - Thot(n))./(thick(n).*Hfg) ;

          tolerancezz(n) = abs(1 - (mevap(n)./mevapA(n)));
          zz = zz+1 ;
        end

        if n == 2
          T(n,1) = Thot(n);
        else
          T(n,1) = T(n-1,1);
        end

        for i = 2:N-1
          T(n,i) = T(n,1) + ((T(n,N) - T(n,1))./(N-1).*(i-1));
        end

      Thot(n) = ((-ks.*pi.*D.*dx.*(T(n,N) - T(n,1))./thick(n)) + mevap(n).*pi.*D.*dx.*Hfg
+ mCphot.*Thot(n-1))./mCphot;

      Tavg(n) = sum(T(n,:) - 273.15)./N;
      wavg(n) = sum(w(n,:))./N;

      T(n,1) = Thot(n);

      tolerancez(n) = abs(1 - ((Thot(n))./(T(n,1))));
      z = z+1;

    end

  end

  error = abs(1 - (Thot(M))/(Thotin));
  Thot = Thot0.*ones(M,1) + Y;
  Y = Y + 0.0001;
  end
```

```
w(n,:) = wavg(n);

%    Well-Mixed #1 - - - - - - - - - - - - - - - - - - - - - - - - - - - - - - - -

   Thot0 = 67.52 + 273.15;              %Vary
   Thot = Thot0.*ones(M,1);
   Y = 0.00001;

   while error > 0.0001

   for n = M*0.5+1:M

      while tolerancez(n) > 0.0001
         T(n,1) = Thot(n);

            while tolerancezz(n) > 0.0001
               mevapA(n) = mevap(n);
               talevapA(n) = mevapA(n)*dx;
               tal(n) = tal(n-1) - talevapA(n);
               dtal(n) = tal(n) - tal(n-1);
               thick(n) = (3*tal(n)*divis/(g*rho)).^(1/3);
               dthick(n) = thick(n) - thick(n-1);

                  for i = 2:N-1
                     u(n,i) = ((rho.*g.*thick(n).^2)./(2*vis)).*(2.*ne(i) - ne(i).^2);
                     v(n,i) = -
1.*((rho*g^2)./(74.*vis^2.*tal(n).^2)).^(1/3).*((thick(n).^2).*(ne(i).^2).*dtal(n))./(L*dx);
                  end

                 for i = 2:N-1

                     aheat(n,i) = ((ne(i).*dthick(n)./(thick(n).*dx)) -
(v(n,i).*L./(u(n,i).*thick(n)))).*dx/dy;
                     bheat(n,i) = (alpha*L./(u(n,i).*thick(n).^2)).*(dx/(dy^2));
                     amass(n,i) = ((ne(i).*dthick(n)./(thick(n).*dx)) -
(v(n,i).*L./(u(n,i).*thick(n)))).*dx/dy;
                     cmass(n,i) = (Dm*L./(u(n,i).*thick(n).^2)).*(dx/(dy^2));

                     Aheat(n,i) = bheat(n,i);
                     Bheat(n,i) = (1 - aheat(n,i) - 2.*bheat(n,i));
                     Cheat(n,i) = aheat(n,i) + bheat(n,i);

                     Amass(n,i) = cmass(n,i);
                     Bmass(n,i) = (1 - amass(n,i) - 2.*cmass(n,i));
                     Cmass(n,i) = amass(n,i) + cmass(n,i);
                  end

                  for i = 2:N-1
```

```
            w(n,i) = Amass(n,i).*w(n-1,i-1) + Bmass(n,i).*w(n-1,i) + Cmass(n,i).*w(n-
1,i+1);
          end

          J = mevapA(n).*thick(n).*dy./(rho*Dm) ;
          w(n,N) = (J + w(n,N-1))./(J + 1) ;

          A(n) = 7.944 - 0.4728.*w(n,N) + 1.847.*w(n,N).^2 - 2.526.*w(n,N).^3 ;
          B(n) = 1653 - 264.9.*w(n,N) + 1158.*w(n,N).^2 - 1497.*w(n,N).^3 ;
          C(n) = 226.7 - 29.01.*w(n,N) + 126.2.*w(n,N).^2 - 164.2.*w(n,N).^3 ;
          T(n,N) = -(B(n)./(log10(P)-A(n))) - C(n) + 273.15 ;
          mevap(n) = -ks.*(T(n,N) - Thot(n))./(thick(n).*Hfg) ;

          tolerancezz(n) = abs(1 - (mevap(n)./mevapA(n)));
          zz = zz+1 ;
        end

        if n == 2
          T(n,1) = Thot(n);
        else
          T(n,1) = T(n-1,1);
        end

        for i = 2:N-1
          T(n,i) = T(n,1) + ((T(n,N) - T(n,1))./(N-1).*(i-1));
        end

      Thot(n) = ((-ks.*pi.*D.*dx.*(T(n,N) - T(n,1))./thick(n)) + mevap(n).*pi.*D.*dx.*Hfg
+ mCphot.*Thot(n-1))./mCphot;

      Tavg(n) = sum(T(n,:) - 273.15)./N;
      wavg(n) = sum(w(n,:))./N;

      T(n,1) = Thot(n);

      tolerancez(n) = abs(1 - ((Thot(n))./(T(n,1))));
      z = z+1;
    end
  end

  error = abs(1 - (Thot(M))/(Thotin));
  Thot = Thot0.*ones(M,1) + Y;
  Y = Y + 0.0001;
  end

% ++++++++++++++++++++++++++++++++++++++++++++++++++++++++++++++++++++++++++

  MWwater = 18.015;          %g/mol
  MWglucose = 180.156;       %g/mol
```

```
%Vapor
  rhoT32_9 = 0.0354 ;
  rhoT45_8 = 0.0682 ;
  % 1 psi = 51.71484 Hg


    %    Change K to oC
    for n = 1:M
      for i = 1:N
        ToC(n,i) = T(n,i) - 273.15;
      end
    end


%++++++++++++++++++++++++++++++++++++++++++++++++++++++++++++++++++++++++++++++

%     Generals
    Tavg(1) = Tin - 273.15;
    wsur = sum(w(:,N))/M;
    Qin = mCphot*(Thot(M) - Thot(1));

      %    Concentration profiles
    for i = 1:N
      wxavg(i) = sum(w(:,i))./M;
      Txavg(i) = sum(T(:,i))./M - 273.15;
    end

                n = 1;
                for i = 1:N
                  u(n,i) = ((rho.*g.*thick(n).^2)./(2*vis)).*(2.*ne(i) - ne(i).^2);
                end

                uin = sum(u(1,:))/N;

  Feed = 4*tal(1)*pi*D*3600;
  Feedwater = (1 - win)*Feed;
  Feedsugar = win*Feed;

  Product = 4*tal(M)*pi*D*3600;

  Evap = Feed - Product;
  Evapratio = Evap/Feedwater*100;
  EvapratioTotal = Evap/Feed*100;

  wout = Feedsugar/Product*100;

  for n = 1:M
    water(n) = (1 - wavg(n)).*tal(n).*pi*D;        %kg/s
    sugar(n) = wavg(n).*tal(n).*pi*D;              %kg/s
  end
```

```
%    Given    lnPsat (kPa) = AA - [BB/(T + CC)] in kelvin for "water"
   AA = 16.3872;
   BB = 3885.7;
   CC = -42.980;
      for n = 1:M
        Psat(n) = exp(AA - (BB./(T(n,N) + CC)))*7.500638;   %1 kPa = 7.500638 mmHg
      end

   for n = 1:M
      molwater(n) = water(n)./MWwater.*1000;
      molglucose(n) = sugar(n)./MWglucose.*1000;

      molfracwaterg(n) = molwater(n)./(molwater(n) + molglucose(n));
      molfracglucose(n) = 1 - molfracwaterg(n);
   end

   for n = 1:M
      molwater(n) = water(n)./MWwater.*1000;
      molglucose(n) = sugar(n)./MWglucose.*1000;

      molfracwaterg(n) = molwater(n)./(molwater(n) + molglucose(n));     %water by glocose
      molfracglucose(n) = 1 - molfracwaterg(n);                          %glucose
   end


   % Activity     Raoult's Law yP = (ac)(x)Psat
   for n = 1:M
      ac(n) = 1./molfracwaterg(n).*P./Psat(n);
      xwater(n) = 40./Psat(n)./ac(n);
   end


%++++++++++++++++++++++++++++++++++++++++++++++++++++++++++++++++++++++++++++++

   %Pressure drop in annular pipe calculation

      %Vapor visvosity from paper (water vapor vis)
      rhovaporin = (0.002617-0.001298)/(311.5-298.39)*(T(2,N)-298.39)+0.001298;
%[mol/L]
      visvaporin = ((10.151-9.703)/(311.5-298.39)*(T(2,N)-298.39) + 9.703 -
1.543*rhovaporin)*10E-6;     %[kg/m.s]

      rhovaporout = (0.002617-0.001298)/(311.5-298.39)*(T(M,N)-298.39)+0.001298;
%[mol/L]
      visvaporout = ((10.151-9.703)/(311.5-298.39)*(T(M,N)-298.39) + 9.703 -
1.543*rhovaporin)*10E-6;     %[kg/m.s]

      rhovapor = rhovaporin/2 + rhovaporout/2;
      visvapor = visvaporin/2 + visvaporout/2;
```

```
% Free volume calculations

residuemass = 4*sum(tal).*pi*D;          %[kg/s]              %Vary++++
residuevolume = residuemass./rho;        %[m3/s]

FreeVolume = pi*Ds^2/4*L - (residuevolume + 4*pi*D^2/4*L);    %[m3/s]

% Vapor
rhoV = ((rhoT45_8 - rhoT32_9)/(45.8-32.9).*(36.15095 - 32.9) + rhoT32_9);
vaporMass = FreeVolume*rhoV;              % Change avg Temp

% Amount in Film
for n = 2:M
   amountWater = 4*(1-wavg).*tal(n).*pi*D;                %Vary++++++++++++++
   amountSugar = 4*(wavg)*tal(n)*pi*D;                    %Vary++++++++++++++
end

%Film
filmtotalWater = sum(amountWater);
filmtotalSugar = sum(amountSugar);

%MOL
molFreeVolume = vaporMass/MWwater;
molFilmWater = filmtotalWater/MWwater;
molFilmSugar = filmtotalSugar/MWglucose;
molFilm = molFilmWater + molFilmSugar;
moltotal = molFreeVolume + molFilmWater + molFilmSugar; %[kmol/s]

%viscosity
visShellin = (vis*molFilm + visvaporin*molFreeVolume)/moltotal;
visShellout = (vis*molFilm + visvaporout*molFreeVolume)/moltotal;
ratiovisShell = visShellin/visShellout;

%Mass and Density
MassShell = residuemass + vaporMass;
rhoShell = (rho*molFilm + rhoV*molFreeVolume)/moltotal;
VShell = MassShell/rhoShell;

% Outside
   TTo = zeros(M,N);
   TTo(M,:) = Ti(M);
   mu = zeros(M,N);
   den = zeros(M,N);
   uu = zeros(M,N);

for n = 1:M
   TTo(n,1) = Ti(n);
end
```

```
  for n = M-1
    for i = 2:N-1
      muu(n,i) = 0.4035E-3 + ((0.354-0.4035)*10^(-4))*(TTo(n+1,i)-273.15-70);
      denn(n,i) = 977.8 + ((971.8-977.8)/10)*(TTo(n+1,i)-273.15-70);
    end
  end

%     Computational fluid dynamics
      den = denn(299,10);
      mu = muu(299,10);
      Areaout = pi*D_D/4;
      Areain = pi*Dsi^2/4;
      vin = mhot/den/Areaout;
      vout = mhot/den/Areain;
      Rein = den*Do*vin/mu;
      Reout = den*Dsi*vout/mu;
      HeatFluxTube = sum(QQ)/(pi*Dti*L);
      HeatFluxTubeUpper = -kwall*(Thott(2)-Tii(2))/Wallthick;

    T(M,1) - 273.15;
    Thot(M)-273.15;

    uin = sum(u(2,:))/N;
    feed = tal0*pi*D*3600*4;
    mevaptotal = sum(mevap).*pi*D*dx*3600*4;
    product = feed - mevaptotal;
    Rate = mevaptotal/feed*100;
    detaT =2*pi*(1.9*0.0254/2)^2*HeatFluxTubeUpper/(mCphot);

%     Pressure Drop Coefficient (zi)
    fzl = 1;
    fal = (280*pi*(b^0.5-0.6)^2 + 0.75)/(4*a*b-pi)/a^1.6;
    zil = fal/Re;
    zi = zil*fzl;

%     We
    s = 1;                          %baffle spacing
    LE = (Ds/2 - rSq - D/2) + PSq;
    AE = s*LE;
    We = VShell/AE;

%     Pressure Drop
    PQ = zi*2*rhoShell*We^2/2;
    fB = 1;
    fL = 1;
    Pdrop =PQ*fL*fB*7.500638;

%     Report

      plot(ab,wavg);
```

```
xlabel ('Non-dimensional y-axis');
ylabel ('Concentration (wt%)');
title ('Concentration of the falling film');
```

BIBLIOGRAHPY

Name: Mr. Chittapol Sooksanit

Date of Birth: 07/11/1995

Address: 12/4 Krungsrinok Road, Mueng Surin Sub-Procince,
Surin Province, Thailand, 32000

E-mail: sportsjamesy@hotmail.com

Academic Background: Petrochemical Engineering, King Mongkut's Institute of Technology Ladkrabang, Bangkok 2014-2017

Math-Science Program, Sirindhorn School, Surin, High School